Holocene Landscape Dynamics and Long-term Population Trends in the Levant

Alessio Palmisano[1], Jessie Woodbridge[2], Neil Roberts[2], Andrew Bevan[1], Ralph Fyfe[2], Stephen Shennan[1], Rachid Cheddadi[3], Raphael Greenberg[4], David Kaniewski[5], Dafna Langgut[6], Suzanne AG Leroy[7], Thomas Litt[8], and Andrea Miebach[8].

1. Institute of Archaeology, University College London, London, UK,
a.palmisano@ucl.ac.uk
2. School of Geography, Earth and Environmental Sciences, University of Plymouth, Plymouth, UK.
3. Institut des Sciences de l'Evolution de Montpellier, Université de Montpellier, CNRS-UM-IRD, Montpellier, France.
4. Department of Archaeology and Ancient Near East Cultures, Tel Aviv University, Tel Aviv, Israel.
5. EcoLab (Laboratoire d'Ecologie Fonctionnelle et Environnement), Université Paul Sabatier, CNRS, Toulouse cedex 9, France.
6. Institute of Archaeology, and the Steinhardt Museum of Natural History, Tel Aviv University, Israel.
7. Aix Marseille Université, CNRS, Ministère de la Culture, LAMPEA, UMR 7269, 5 rue du Château de l'Horloge, 13094, Aix-en-Provence, France.
8. Steinmann Institute for Geology, Mineralogy, and Paleontology, University of Bonn, Bonn, Germany.

Abstract
This paper explores long-term trends in human population and vegetation change in the Levant from the Early to the Late Holocene in order to assess when and how human impact has shaped the region's landscapes over the millennia. To do so, we employed multiple proxies and compared archaeological, pollen and palaeoclimate data within a multi-scalar approach in order to assess how Holocene landscape dynamics change at different geographical scales. We based our analysis on 14 fossil pollen sequences and applied a hierarchical agglomerative clustering and community classification in order to define groups of vegetation types (e.g. grassland, wetland, woodland, etc.). Human impact on the landscape has been assessed by the analysis of pollen indicator groups. Archaeological settlement data and Summed Probability Distribution (SPD) of radiocarbon dates have been used to reconstruct long-term demographic trends. In this study, for the first time, the evolution of the human population is estimated statistically and compared to environmental proxies for assessing the interplay of biotic and abiotic factors in shaping the Holocene landscapes in the Levant.

Keywords
Levant, Archaeology, Demography, Pollen, Vegetation, Climate, Settlement Patterns

1. Introduction
The Levant represents an excellent case study for investigating the impact of anthropogenic activity on landscape transformation and land-use change throughout the Holocene. This area, which saw the earliest onset of agriculture and a complex economy, the emergence of urban systems and their collapse, the rise and fall of regional kingdoms, and the domination by vast empires over the region, is a mosaic of different cultural and environmental landscapes (Gophna and Portugali 1988; Finkelstein 1995 and 2013; Greenberg 2002; Rosen 2007; Savage *et al.* 2007; Finlayson and Warren 2010; Asouti *et al.* 2015; Enzel and Bar-Yosef 2017; Fall *et al.* 2018). These landscapes are linked in certain ways, but ultimately can be shown to have followed varied socio-ecological trajectories (Bar-Yosef and Belfer-Cohen 2002; Issar and Zohar 2004; Cordova 2007; Rosen 2007; Rambeau 2010; Philip 2011; Langgut *et al.* 2015; Porter 2016; Kaniewski *et al.* 2017; Rosen and

Rosen 2017; Lu *et al.* 2017; Roberts *et al.* 2018). Recent studies have shown that population size substantially increased at the beginning of the Holocene with the introduction of farming economies and ameliorated climatic conditions, while population levels were lower when hunter-gatherers were still active in the Levant (cf. Goring-Morris and Belfer-Cohen 2010; Maher *et al.* 2011; Borrel *et al.* 2015; Roberts *et al.* 2018). A higher rate of population growth, characterized by patterns of booms and busts, occurred with the rise of the earliest urban societies in the Bronze Age and peaked in the Late Holocene with the establishment of Iron Age territorial kingdoms and the rule over the region by vast empires (e.g. Assyrian, Persian, Babylonian, Roman, etc.; cf. Finkelstein 1996 and 1998; Bar 2004; Falconer and Savage 2009; Greenberg 2017). The regional archaeological records reflect these processes and events, demonstrating sharp settlement fluctuations and episodes of destruction. In the Late Holocene, the thriving of population, often nucleated in large urban centres demanding agricultural surplus from the surrounding intensively farmed rural hinterland, led to heavy anthropogenised landscapes (Neumann *et al.* 2007; Finkelstein and Langgut 2018).

In this perspective, scholars have developed a research agenda addressing how population growth contributed to transforming the environment from nature-dominated to culturally modified by making use of pollen-based reconstruction of Holocene vegetation change (see Butlin and Roberts 1995; Hajar et al. 2010; Kaniewski *et al.* 2013; Langgut *et al.* 2013-2016; Roberts *et al.* 2011 and 2018). Although human activity could have altered the local landscape via land management practices such as agriculture, grazing and burning (Roberts *et al.* 2011), pollen data suggest that Early Holocene regional composition of woodland and landscape openness in the Levant were mainly linked to natural drivers (van Zeist and Bottema 1991; Djamali *et al.* 2010; Litt *et al.* 2012; Cheddadi and Khater 2016). Instead, a strong human impact on vegetation starts being more evident from the Chalcolithic and Bronze Age onwards and peaked in the Roman and Byzantine periods (see Schwab *et al.* 2004; Hajar *et al.* 2010; Langgut *et al.* 2013 and 2016; Izdebski *et al.* 2016a; Schiebel and Litt 2017). Overall, the Holocene vegetation changes in the Levant are to be interpreted as the results of multiple factors interplaying with each other such as climate events, ecological dynamics and anthropogenic impacts (cf. Rosen 2007; Kaniewski *et al.* 2008; Roberts *et al.* 2011). Likewise, episodes of population increase punctuated by periods of stagnation and decrease could be related to multiple causes not necessarily mutually exclusive such as climate change, migrations, warfare, exceeding carrying capacity of the land, environmental disasters, etc. (Leroy 2006; Rosen 2007; Leroy *et al.* 2010).

With these premises in mind, estimating Holocene landscape dynamics and population fluctuations over the *longue durée* and assessing their relationships is pivotal for how we understand cultural and environmental change. Most studies concerning human impact on the landscape during the Holocene in the Levant have used a limited corpus of archaeological evidence or have focused on assessing human and environmental responses to one or more major rapid climate changes (e.g. the so-called 9.4 ka, 8.2 ka, 4.2 ka and 3.2 ka cal. yr. BP events) and within well-defined cultural periods. In this work, we will draw upon a large corpus of archaeological data (in the form of archaeological settlement data and radiocarbon dates) and pollen records available in the Levant and assess how the impact of anthropogenic and natural factors on the landscape varies significantly by region and depends, in part, on the longer-run socio-ecological dynamics prevailing in different areas from the Early to the Late Holocene (ca. 11,700 – 500 cal. yr. BP).

The advantage of this multi-proxy approach is that the divergences and convergences among the patterns defined by each archaeological and environmental proxy will provide powerful insights and a wider range of explanations in describing demographic and vegetation change both throughout the Holocene time span as a whole and in particular sub-periods. In addition, we will use a multi-scalar approach to detect specific patterns on local scales (North Levant, Transjordan, Cisjordan) and to tackle possible misunderstandings derived from analysing data just on a single scale of analysis. Furthermore, we compare the pollen and archaeological data with paleoclimate records in order to assess the relative impact of climate and human population size on the Holocene vegetation composition in the Levant (Izdebski *et al.* 2016b).

2. Geographical setting and materials

2.1 The study area

The portion of the Levant examined here covers around 65,000 sq. km, encompassing present-day Lebanon, Israel, the West Bank and part of western Jordan and south-western Syria (Fig. 1). This region can be subdivided into four geographical units: Lower North Levant, Cisjordan highlands (i.e. West Bank) and lowlands, and Transjordan (Fig. 1). The spatial coverage of the present study area has been selected (1) according to the regions where a sufficiently high intensity of archaeological excavations and surveys have been conducted, and (2) because of the need to provide a coherent framework both spatially and chronologically for analysing comparatively archaeological data and pollen records.

The area under study shows a varied topography that moving from west to east, includes a landscape of coastlands and plains, the mountain ranges of Lebanon and Anti-Lebanon in the north, the Cisjordan highlands in the south, and the Syrian and Transjordan deserts to the east of the Syro-African Rift valley (Suriano 2013, 14-20). The altitudinal gradient ranging from the highest peak of the Qurnat as Sawda' (3,088 m above mean sea level) in Lebanon to the lowest point in the Dead Sea Rift (413 m below mean seal level) results in marked differences in terms of climate and vegetation composition (Zohari 1962 and 1973; Danin 1988). Average annual rainfall shows a latitudinal gradient with values exceeding 1000 mm in the northern mountain chains of Lebanon to approximately 100 mm at the shores of the Dead Sea (Ziv et *al.* 2006; Cheddadi and Khater 2016, 147-148). As a result, the present study area is sub-divided into three different vegetation zones (cf. Danin 1988; Langgut et al 2014, 282-283; Schiebel and Litt 2017, Fig. 2a): 1) a desert (Saharo-Arabian) territory along the shores of the Dead Sea and in the Arava Valley characterized by Chenopodiaceae plants; 2) a semi-desert (Irano-Turanian) zone distributed along the eastern slopes of Cisjordan highlands and in the Moab plateau; 3) and a Mediterranean vegetation dominated by maquis and evergreen and deciduous oaks over Cisjordan, Lower North Levant and large parts of the Transjordanian plateau.

2.2 Archaeological data

The archaeological datasets (archaeological settlement data and radiocarbon dates) have been collected as exhaustively as possible via harmonisation of existing online databases and both electronic and print publications to create two georeferenced databases (unprojected LatLon coordinate system, WGS84 datum), one for radiocarbon dates (Fig. 1a) and one for archaeological sites (Fig. 1b). A total of 2,173 uncalibrated radiocarbon dates have been identified from 230 sites and either collected from several existing online databases in some cases (EUROEVOL, RADON,

EX ORIENTE) or more often added from a wide range of publications (see Supplemental material 1 for a full list of sources; Fig. 1a). This number exceeds the suggested minimum threshold of 200-500 to produce reliable Summed Probability Distribution (SPD) of radiocarbon dates with reduced statistical fluctuation for a time interval of 10,000 years (cf. Michczyńska and Pazdur 2004; Michczyńska et al. 2007; Williams 2012, 580-581). All of these radiocarbon dates come from archaeological contexts, with the majority being samples of bone, charcoal and wood. Radiocarbon dates obtained from marine samples such as shell have been removed (and are not part of the above total) in order to avoid complicating issues arising from unknown or poorly understood marine reservoir offsets.

[Insert **Figure 1** about here]

To create the database of archaeological sites used below we conducted a comprehensive synthesis, and standardisation of Holocene settlement data from two online databases which represent an excellent source of more than 47,000 sites across the Levant: 1) The Digital Archaeological Atlas of the Holy Land (Savage and Levy 2014)[1]; 2) The West Bank and East Jerusalem Archaeological Database (Greenberg and Keinan 2009)[2]. Settlement data were recorded as geo-referenced points per cultural period. The use of the term 'period' here refers to familiar archaeological episodes in the region such as Chalcolithic, Early Bronze Age, Iron Age, etc. These cultural units were found to be the most common level of aggregation and standardization, but were typically expressed without any absolute calendric dates. By recording both the stated cultural period and approximate estimated start and end dates in calendrical years, we have sought to provide maximum comparative potential across archaeological sites from different regions, standardizing period-based terminology where necessary (see Table 1 for the chronological scheme adopted). One major caveat is that the estimated site extent per cultural period was not recorded for all the sites stored in the two online databases. As a consequence, in this work we use site counts as a proxy for population. A total of 20,688 sites and 66,183 occupation phases have been collected using the above approach (with these numbers showing that most sites experienced multiple periods of occupation; see Fig. 1b).

[Insert **Table 1** about here]

2.3 Pollen data

The fossil pollen dataset includes 14 sequences from 13 sites (Fig. 1 and Table 2), and the modern pollen dataset includes 35 surface pollen samples from locations across the Southern Levant. The pollen data primarily derive from collaborators (Table 2), and the European modern (Davis et al., 2013) and fossil pollen databases (Leydet et al., 2007-2017). These records formed part of a Mediterranean-wide analysis of vegetation change based on cluster analysis and community classification (see Woodbridge et al., 2018, and Fyfe et al., 2018 for further details). Only pollen sequences with reliable chronologies were selected for analysis (see Giesecke et al., 2014). Hence, new chronologies were made for collaborators' datasets and confirmed with the original authors. This allows us a more reliable control on the reconstruction of vegetation change than has been possible in previous studies.

[1] The Digital Archaeological Atlas of the Holy Land (DAAHL) was a project conducted by S. H. Savage and T. E. Levy and contains more than 47,000 sites from Cyprus, Israel, Jordan, Lebanon, the Sinai Peninsula, and the West Bank: https://daahl.ucsd.edu/DAAHL/Home.php.

[2] The West Bank and East Jerusalem Database was created by R. Greenberg and A. Keinan and includes approximately 6,000 surveyed sites and 1,000 excavated sites: http://digitallibrary.usc.edu/cdm/landingpage/collection/p15799coll74.

2.4 Palaeoclimate data

The palaeoclimate data derive from analyses of caves speleothem archives at Soreq and Jeita (Fig. 1) and provide past precipitation proxies inferred from stable isotopes $\delta^{18}O$ (Bar-Matthews *et al.* 1999 and 2003; Cheng *et al.* 2015). The isotope values of these two datasets have been normalised around their Holocene's mean and standard deviation to produce a z-score (Fig. 6), which has been transformed in order to have higher positive values indicating wetter climatic conditions and lower negative values for dry climate.

[Insert **Table 2** about here]

3. Methods

3.1 Demographic trends from archaeological data

Population estimates build on the assumption that an observable density of archaeological evidence over time and across a study region is proportional to population (see Drennan 2015 *et al.* for a good overview). In this work, we use two types of archaeological data as proxies for estimating population fluctuations over the long run: 1) SPDs of radiocarbon dates; 2) settlement data including site counts.

We reduced the potential "wealth-bias" of oversampling specific site-phases by aggregating uncalibrated radiocarbon dates from the same site that are within 100 years of each other and dividing by the number of dates that fall in this bin (Timpson *et al.* 2014). Dates having a gap of at least 100 years from the previous one are assigned to a new bin. In this step, our 2,173 radiocarbon dates have been grouped into 837 bins. The probabilities from each calibrated date are combined to produce a summed probability distribution (SPD). Following previous works (Williams 2012; Weninger *et al.* 2009 and 2015) demonstrating that normalized calibrated dates emphasize narrow artificial peaks in SPDs due to steepening portions of the radiocarbon calibration curve, we opted to use unnormalised dates prior to summation and calibrated via IntCal13 curve (Reimer et al. 2013; see former applications in Palmisano *et al.* 2017; Bevan *et al.* 2017; Roberts *et al.* 2018). Consequently, a logistic null model representing expected population growth and plateau has been fitted to the observed SPD in order to produce a 95% confidence envelope (composed of 1,000 random SPDs) and to statistically test if the observed pattern significantly departs from this model (for a detailed explanation of the method, see Timpson et al. 2014, 555-556; Bevan *et al.* 2017; Crema and Bevan 2018). Deviations above and below the 95% confidence limits of the envelope respectively indicate periods of population growth and decline greater than expected according to a logistic model of population growth. This theoretical null model of population change builds on the assumption that a population's per capita growth rate decreases to zero as population size approaches a maximum imposed by limited resources in the environment as there might be an upper bound to pre-Iron Age population growth. However, It is important to bear in mind that a logistic model cannot be considered strictly as a realistic model for population growth, but rather as an elementary model useful for quantitatively testing population fluctuations (cf. Turchin 2001). In this case, we preferred a logistic model to other possible null-models (e.g. uniform, exponential) given the observed shape of SPD of radiocarbon dates in our study area (see Fig. 2a).

We calculated the sites count for 200-year time slices starting with $period_{t1}$ (12000 -11800 cal. yr. BP) and ending with $period_{t57}$ (800-600 cal. yr. BP). Bearing in mind that archaeological cultures

result in larger or shorter time spans according to the dating precision of archaeological artefacts, we applied a probabilistic approach known as aoristic analysis to deal with the temporal uncertainty of occupation periods (for a more detailed explanation of the methodology see Crema *et al.* 2010, 1118-1121; Crema 2012, 446-448; Palmisano *et al.* 2017, 63-65). In addition, to mitigate the discrepancy between wide chronological uncertainties and narrower likely site durations, we applied Monte Carlo methods to generate randomised start of occupation periods for sites with low-resolution information (cf. Crema 2012, 450-451; Kolář et al. 2016, 518-519; Orton et al. 2017, 5-6; Palmisano *et al.* 2017, 63-64). The resulting probabilistic distributions of site frequencies through time, based on the aoristic sums and Monte Carlo simulations, provide useful comparisons with the raw site frequency data.

3.2 Pollen inferred land cover vegetation

Pollen count data have been summed into 200-year time windows through the Holocene and vegetation cluster group change is presented as the percentage of samples assigned to each vegetation type. Descriptions of the methodological approaches developed and applied to the pollen datasets are provided in Woodbridge *et al.* (2018) and Fyfe *et al.* (2018).

Simpson's diversity index has also been applied to the data to explore major changes and shifts in diversity patterns over time. Simpson's index has been calculated for each pollen sample using pollen percentage data. This index takes both species richness and evenness into account and is often used to explore diversity change in pollen datasets (e.g. Morris *et al.* 2014; Woodbridge *et al*., 2018). Values for a number of pollen indicator groups have been calculated. This includes: Arboreal Pollen (AP%), an Anthropogenic Pollen Index (API: *Artemisia, Centaurea*, Cichorioideae, *Plantago*, cereals, *Urtica* and *Trifolium* type; Mercuri et al., 2013a), an indicator group for cultivated trees (OJC: *Olea, Juglans, Castanea*; Mercuri et al., 2013b) with the addition of *Vitis* (OJCV), and a group of pastoral land use indicators (*Artemisia*, Chenopodiaceae, *Plantago lanceolata* and *Plantago major/media*, Asteroideae, Cichorioideae, *Cirsium*-type, *Galium*-type, Ranunculaceae and *Potentilla*-type; adapted from Mazier et al., 2006 and 2009). An additional pollen indicator group including ruderal weeds (Polygonaceae, Urticaceae, *Plantago lanceolata*) and grazing-resistant plants such as *Cirsium, Carduus* and different species of *Centaurea* (*C. nigra, C. solsticialis* and
C. cyanus) has been calculated (adapted from Langgut *et al.* 2014). Because this latter group encompasses together secondary anthropogenic (ruderal weeds) and grazing indicators, an increase of these taxa reflect more generally a more intense human impact on the vegetation such as woodland clearance, increase of pasture lands, building activity (e.g. settlements, mining, roads, etc.) and agriculture (e.g. terracing, abandoned fields, irrigation, etc.).

It is important to point out that the regional pastoral indicators group was developed using the same grouping of taxa used in France, so is less informative about landscape change in the Levant, but has been included to allow comparisons between different case study regions within a Mediterranean-wide synthesis (Roberts *et al*., in press).

Amalgamated results are shown for the entire region and the Arboreal Pollen (%), OJCV index, API and regional pastoral indicators are also presented for individual sites. The Arboreal Pollen (%) does not include the cultivated trees. Indicator groups are useful to assess the anthropogenic impact on landscape tranformation across time. Although the indicator groups are based on literature that describe the taxa as 'anthropogenic indicators', some of these taxa are also indicators of natural vegetation types, for example, Chenopodiaceae Asteroideae, Cichorioideae indicate natural steppe vegetation.

4. Results

4.1 Demographic trends

Figure 2a shows the SPD of 2,173 unnormalised calibrated radiocarbon dates from 12000 to 2500 cal. yr. BP compared with a 95% confidence envelop for a logistic null model. Deviations above (in red) and below (in blue) the null model represent respectively patterns of population growth and decline beyond than expected under a long-term logistic demographic trend. The observed SPD (black solid line) shows a significant overall departure from the envelope of the logistic model (global *p*-value= 0.001).

From the end of the Younger Dryas at ~11700 cal. yr. BP, corresponding to the onset of the Holocene, a steady increase of population occurs until 9500 cal. yr. BP. Then, population starts decreasing during the PPNB and falls below the null model in the PNA (8400 – 7600 cal. yr. BP). The population rises in the late PNB and in the Chalcolithic, and it reaches a peak above that expected between 6100 and 5800 cal. yr. BP. The Bronze Age is characterized by peaks of population in the EBA (5300 – 4600 cal. yr. BP) and MBA (this one is not statistically significant) punctuated by significant population decrease in the IBA (4200 – 4000 cal. yr. BP) and in the LBA (3400 – 3200 cal. yr. BP). A further dramatic increase of population occurs at the start of the Iron Age (~3100 – 2800 cal. yr. BP). After this period, the radiocarbon population proxy gradually decreases until the end of the Iron Age. In addition, it is important to point out that the later periods (after 2500 cal. yr. BP) have been excluded in the present analysis because the SPD of radiocarbon dates massively underestimates a widely-agreed and widely-evidenced boom in population during the Roman and Byzantine periods (Broshi 1979; Bar 2004; Geva 2014). This is due to the reliance by most Roman and Byzantine archaeologists on typo-chronological schemes defined by short-lived pottery types and coins for dating rather than using radiocarbon samples. Furthermore, a caveat in the patterns described by the SPD of radiocarbon dates is represented by the fact that certain chronological periods are more likely to be sampled than others. For instance, the significant growth of population during the EBA and the IA could reflect research biases related to the interest of many archaeologists in providing a better chronology for the EBA sub-periods and the LBA/IA transition (cf. Mazar and Bronk Ramsey 2008 and 2010; Finkelstein and Piasetzky 2010 and 2011; Braun 2012; Regev *et al.* 2012).

Figure 2b shows the frequency per 200-year time-block of 66,183 site occupation phases from 20,688 sites. Three different versions have been derived from archaeological settlement data to infer population dynamics over the long run: raw site counts, aoristic sum and randomised start date of site-phase. The results show for all three proxies an increase of population from the onset of the early Holocene (at least more pronounced for the site counts) and a decrease during the PNA (~ 8500 – 7500 cal. yr. BP). Then, population starts growing again during the Chalcolithic and is characterized by patterns of boom and bust during the Bronze Age (see Figure 2c). The results show a substantial growth of population in the Iron Age (~3100 – 2700 cal. yr. BP), in the Roman-Byzantine period (~ 2000 – 1300 cal. yr. BP), and in the Middle Islamic (900 – 600 cal. yr. BP). These episodes are punctuated by a population decline in the Babylonian-Persian period (~ 2500 – 2300 cal. yr. BP) and in the Early Islamic (1300 – 900 cal. yr. BP).

[Insert **Figure 2** about here]

Figure 3 shows the regionally subdivided SPD of unnormalised radiocarbon dates compared against the pan-regional trend (grey envelope) described above. In this case, we assess to which degree the demographic patterns of each sub-region depart from the pan-regional trend via a permutation test

(see Crema *et al.* 2016 for a detailed description of the methodology). Such a technique also deal with the issues represented by the size of the samples, as the resulting grey envelopes of the pan-regional trend are larger in those sub-regions with less radiocarbon dates (see Fig. 3). Therefore, the grey envelopes are larger because more uncertainty. It is important to emphasise that this approach allow us to compare relative change through time of the SPDs (and so the proportional change of population) within each sub-region and not their differences as absolute magnitudes in terms of population. Cisjordan lowlands (Fig. 3b) and highlands (Fig. 3c) show significant departures from the pan-regional trend (p-value < 0.05), while the Lower North Levant (Fig. 3a) and Transjordan (Fig. 3d) do not depart significantly from the overall shape of the pan-regional trend (p-value > 0.25). Although the latter ones have global demographic trends similar with the pan-regional one, they still show some local deviations. In fact, in the Lower North Levant (Fig. 3a) the population density is significantly above the pan-regional pattern in the PPNB (9700 – 9500 cal. yr. BP), in the PNA (7700 – 7500 cal. yr. BP) and in the EBA (4800 – 4500 cal. yr. BP). Transjordan (Fig. 3d) shows short-local deviations above the general trends through the PNA and a significant negative deviation in the IA (~3200 – 2800 cal. yr. BP). In the Cisjordan lowlands (Fig. 3b) the population trend is flat and lies below the pan-regional confidence envelope in the PPNA (11400 – 11100 cal. yr. BP) and significantly exceeds the global pattern in the IA (~3200 – 3100 cal. yr. BP). The Cisjordan highlands (Fig. 3c) are characterized by a local positive demographic departure in the PPNA (12000 – 10800 cal. yr. BP) and a significant decrease below the pan-regional trend in the PNA (~7900 – 7400 cal. yr. BP).

[Insert **Figure 3** about here]

Fig. 4 shows settlement dynamics in the four sub-regions. In all regions, population as inferred by this particular proxy seems to increase since the beginning of the Holocene and then is stable until the PNA (~8500 – 7500 cal. yr. BP), at which time it decreases in Cisjordan and (Fig. 4b-c) Transjordan (Fig. 4d). Then, population starts increasing rapidly in the Chalcolithic and Bronze Age, and peaks during the Iron Age and Roman-Byzantine periods. Episodes of marked population decline occur in all four regions during the Late Bronze Age (~3300 – 3100 cal. yr. BP) and in the Early Islamic (~1200 – 800 cal. yr. BP).
Unlike the radiocarbon dates, the three proxies derived from archaeological settlement data (raw count, aoristic sum, and randomized start date) provide a better coverage both chronologically and spatially in the area under investigation, as they are the results of intensive and extensive archaeological surveys carried out across the Levant. A pairwise Spearman's correlations between all demographic proxies show that they are strongly correlated and describe similar patterns (Table 3). In particular, the demographic trends defined by SPD of radiocarbon dates are strongly correlated with the ones derived from the archaeological settlement data ($r > 0.68$) during the period from 12000 to 2600 cal. yr. BP.

[Insert **Figure 4** about here]

4.2 Land cover vegetation change

The 14 pollen records from 13 sites have been used to infer Holocene vegetation change in the study area as a whole. Unfortunately, the patchiness of data in terms of spatial and chronological coverage of the records does not allow us to subdivide vegetation cluster group trends into two or more sub-regions, as patterns are highly influenced by a small number of sites. The pollen samples

have been divided into 16 pollen-inferred vegetation clusters via hierarchical clustering according to the classification of Mediterranean pollen assemblages described by Fyfe *et al.* (2018) and Woodbridge *et al.* (2018). In the Levant, not all the 16 vegetation clusters are represented (see Fig. 5). The main groups are 1.1 (sclerophyllous parkland), 1.3 (steppe parkland), and 1.4 (parkland/grassland). Moderately prominent are the groups 1.2 (evergreen shrubland: *Oleaceae*) and 2.0 (evergreen shurbland: *Quercus*). Cluster 1, which is the aggregation of four groups, is the dominant vegetation feature across the whole Holocene. This cluster represents open and human-modified vegetation and includes several constant taxa such as Poaceae, Chenopodiaceae, *Artemisia*, *Quercus*, and Asteraceae. Evergreen shrubland (Oleaceae, group 1.2) starts appearing at 7000 cal. yr. BP and reaches its peak (~ 30%) at around 6500 cal. yr. BP. Since then, it gradually decreases and disappears between 4500 cal. yr. BP and 2400 cal. yr. BP. It starts increasing again at ~2000 cal. yr. BP and constantly represents the 20-25 % of the pollen assemblage until the 1000 cal. yr. BP before declining again. Evergreen shrubland (*Quercus*) is recorded between 10500 and 9800 cal. yr. BP and then from 6400 cal. yr. BP onwards until the present. Deciduous oak parklands and woodlands (cluster 6.1 and 6.2) are recorded only between 11000 and 9200 cal. yr. BP.

[Insert **Figure 5** about here]

Arboreal Pollen (AP%) fluctuated between 15 and 45% throughout the Holocene with a gradual decline from 10000 to 6600 cal. yr. BP (Fig. 6). After this, the arboreal pollen percent starts increasing steadily until 4000 cal. yr. BP and it gradually decreases until 1500 cal. yr. BP. Following this time, it grows steadily (Fig. 6). A marked increase of cultivated trees (*Olea*, *Juglans*, *Castanea* and *Vitis*) occurs between 6500 and 1000 cal. yr. BP as indicated by the OJCV index (Fig. 6). This general trend is punctuated by a decline of cultivated trees between 4000 and 1500 cal. yr. BP, and from 1000 cal. yr. BP onwards. It is important to point out that the dominant taxa in the OJCV index in this region is represented by *Olea*. The API indicates an increase of anthropogenic activity from 9000 to 6500 cal. yr. BP, and a gradual decrease after this time. The inferred anthropogenic activity starts increasing again from 4000 cal. yr. BP onwards. Similar trends throughout the Holocene occur also for the regional pastoral indicators. The ruderal and gazing resistant plants suggests an increase of human pressure on the natural environment between 11000 and 9500 BP, followed by a sharp decline until 6500 BP. After this, the ruderal weeds and grazing resistant plants increase again until 4500 BP, and then starts decrease gradually until the modern era (Fig. 6). However, it is important to point out that the regional pattern provided by this latter indicator is mostly skewed by the pollen assemblage from Al Jourd (see Fig.9), which is characterised by a substantial peak during the 5500-4500 BP reflecting a stronger human activity such as oak and cedar deforestation (Hajar et al. 2010). Simpson's index suggests that landscape diversity increased since the Early Holocene and increased further from 2500 cal. yr. BP onwards.

[Insert **Figure 6** about here]

4.3 Comparing landscape dynamics vs. population proxies

The demographic proxies (SPD of radiocarbon dates, aoristic sum, and raw count) and the z-score of the palaeoclimate records are binned into 200-year time slices to match the time windows used in the analysis of pollen sequences. The use of a 200-year time window for all the proxies is justified by the fact that this is the finest chronological resolution provided by the pollen data. We also calculated the median of the envelope of the randomised start date of sites, which is the result of

1,000 randomised runs, and binned this into 200-year time slices. This step provides a measurement comparable with the other demographic and environmental proxies. A Spearman's Rank correlation matrix between pollen indicators, archaeological demographic proxies and palaeoclimate records for the period from 11000 to 600 cal. yr. BP is given in Table 3. Pairwise Spearman's correlations between SPD of radiocarbon dates and all other proxies have been calculated in a shorter time span between 11000 and 2600 cal. yr. BP, because after this time the radiocarbon dates are not a good proxy for inferring demographic trends as discussed above. Spearman's correlations between all demographic proxies indicate strong positive correlation (p-value < 0.001) and suggest that the archaeological data depict similar population dynamics over the long run. The palaeoclimate records are negatively correlated with all demographic proxies and pollen indicators such as AP percent and OJCV index. Instead, the API and the regional pastoral indicators show a positive relationship with climate proxies. The clearest significant correlations (p-value < 0.001) are between the demographic proxies and OJCV index, which implies that cultivated trees were more abundant when there was a higher population. Regional pastoral indicators are negatively correlated with population, while the AP percentage is positively related with demographic proxies. The Simpson Index does not show any correlation with the demographic proxies. The positive correlation between all demographic proxies and AP percent suggests that demographic growth is not associated with a decline of trees as would be expected in the case of negative correlation. Positive correlations between ruderal weeds + grazing resistant plants and demographic proxies indicate that disturbed lands are a result of human activity. The palaeoclimate records from Soreq and Jeita caves are positively correlated (p-value < 0.001) throughout the Holocene (Table 3). Their averaged z-scores indicate wetter conditions in the Early and Mid-Holocene (until ~ 7000 cal. yr. BP), which is followed by a drier climate until ~ 1000 cal. yr. BP.

[Insert **Table 3** about here]

However, the results described here only provide us with an overall picture of long-term trends, by treating the Holocene as a whole. Instead, in order to have a better understanding of the human impact on the landscape, we have adopted a moving window approach. The advantage of this approach is to to identify periods of correspondence and divergence between human population size, vegetation change and palaeoclimate records over shorter time periods from the Early to the Late Holocene (11000 – 600 cal. yr. BP). Thus, a 2000 year-time moving window Spearman's correlation has been used, with ten 200-year bins in each time window (see Supplemental Material 2: Tables S1-S10). In addition, cross correlation analysis has been performed in order to assess if one time series "causes" changes in another and if they occur with a defined time-lag between each other. Here, the time lag unit is 200 years. Cross-correlation values have been indicated in Supplemental Material 2 (Tables S1-S10) only for those 2000-year time windows showing significant Spearman's correlations.

The results in Supplemental Material 2 (Table S1) show that population is positively correlated with AP percentage (trees and shrubs) during the Mid-Holocene. Most of the correlations have a lag equal to 0 indicating contemporaneity between demographic trends and vegetation change. This is also due to the fact that our 200-year resolution is quite coarse to assess time lags between demographic proxies and pollen indicators. The results in Supplemental Material 2 (Table S2) show a strong positive correlation between demographic trends and OJCV pollen during the Mid-Holocene, encompassing those periods when population starts increasing from 7000 cal. yr. BP

onwards. Also in this case almost all correlations have a lag equal to 0. Other strong positive correlations occur in the Late Holocene (from 3800 cal. yr. BP onwards). Negative correlation occurs between demographic proxies and API and regional pastoral indicators (Supplemental Material 2: Tables S3 and S4) in the Mid-Holocene, while they are positively correlated in the Late Holocene. In this case, some cross correlations have negative lags (-1), indicating that the increase of population anticipates by 200 years the increase of those taxa related to the anthropogenic activity and pastoral land use. Secondary anthropogenic indicators (ruderal weeds + grazing resistant plants) show positive correlation with demographic proxies during the Middle Holocene (~8600-4400 BP; Supplemental Material 2: Table S5). Not particularly strong correlations occur between population and Simpson's diversity Index (Supplemental Material 2: Table S6). The pollen indicators AP percentage and OJCV are negatively correlated with the palaeoclimate records in the Mid-Holocene, indicating that these pollen taxa groups decreased despite wetter climatic conditions and increased when climate was drier (Supplemental Material 2: Tables S7 and S8). The API index shows a strong positive correlation during the Mid-Holocene (~ 7800 – 4600 cal. yr. BP) and a negative correlation during the Late Holocene (~ 4000 – 1600 cal. yr. BP) with palaeoclimate records from Jeita cave (Supplemental Material 2: Table S8). This indicates that anthropogenic pollen indicators decreased with drier climatic conditions during the Mid-Holocene and increased despite unfavourable hydroclimatic trends occurring between 4000 and 1600 cal. yr. BP. The regional pastoral indicators are positively correlated with the palaeoclimate proxy from Jeita cave during the Early and Mid-Holocene (Supplemental Material 2: Table S8). The ruderal weeds + grazing resistant plants show no significant correlations with the paleoclimate records from Soreq's cave and are negatively correlated in the Early and Mid-Holocene with the climate trends inferred from Jeita's cave speleothem records.

The archaeological proxies from Southern Levant show negative correlation with the palaeoclimate records from Soreq cave (Supplemental Material 2: Table S9), except for those windows encompassing Early Holocene (between 11000 and 9000 cal. yr. BP) and Late Holocene (4200 – 2200 cal. yr. BP). In this latter case, we have a correlation with a positive time lag (+1) indicating that a decline of population is delayed by 200 years and represents a worsening of hydroclimate conditions. A pattern similar to the one described above occurs between demographic proxies from Lower North Levant and the palaeoclimate records from Jeita cave (Supplemental Material 2: Table S10).
However, it is important to bear in mind that in this study we provide some general trends on a broad chronological scale of analysis. The interplay of human and environmental dynamics is difficult to disentangle with a 200-year resolution and micro-regional socio-ecological trajectories are not discernible at the spatial scale of analysis adopted in the present paper.

5. Discussion: Socio-Environmental trajectories from the Early to the Late Holocene

5.1 The Pre-Pottery Neolithic and Pottery Neolithic (ca. 11750 – 6450 cal. yr. BP / 9800 – 4500 BCE)

The Pre-Pottery Neolithic A (PPNA) is the period when people started living in sedentary communities and practicing farming activities, although it is still debated as to whether domestication of crops and animals occurred at this time (Colledge 1998; Colledge *et al.* 2004). However, the transition from a hunter-gatherer economy to sedentary agriculture occurred gradually

and unevenly in time and space (Horwitz et al. 2000; Vrydaghs and Denham 2007; Finlayson 2013). In the later Pre-Pottery Neolithic B (PPNB), a full development of the Neolithic lifestyle took place with an extensive use of crops and livestock management (Asouti and Fuller 2012), which culminated with large nucleated settlements such as Jericho and Yiftahel in Cisjordan, 'Ain Ghazal and 'Ain Jammam in Transjordan, and Tell Ramad in Syria (Bienert 2004; Goring Morris and Belfer-Cohen 2013). The wetter climatic conditions in the Early Holocene could have triggered high-risk but high-yield subsistence strategies, which coincide with the first increase in population from ~ 11700 until 9500 cal. yr. BP (Roberts *et al.* 2018; see Fig. 2a, Supplemental Material 2: Tables S9-10). Given the stable warm and wet climatic conditions, the decrease in population in the late PPNB from 9500 cal. yr. BP onwards is perhaps endogenous and related to the depletion and overexploitation of resources and the exceeded carrying capacity of the landscape (Goring-Morris and Belfer-Cohen 2010; Finlayson 2013, 130). Alternatively, the pronounced sub-centennial rainfall fluctuations between moist and dry conditions (not visible here in the 200-year averaged z-scores of the climate records from Jeita and Soreq's caves) and a general decrease of the Dead Sea level suggest less favourable climate trends between ~9500 to 7000 cal. yr. BP, which could have affected the fragile socio-economic systems of the Levantine community (Bar-Yosef 2002; Stein *et al*. 2010). A decrease in population occurred in Northern Levant and Cisjordan (Fig. 3a-c), while the Transjordan communities did not experience a break in the occupation (cf. Rollefson 2001, 86; Betts 2013, 178; see Fig. 3d).

The Early Holocene landscape shows the predominance of steppe and parkland/grassland vegetation, (clusters 1.1, 1.3-4) which could be the result of both anthropogenic activity and climate conditions. An increase of AP percentage is evident from the onset of the Holocene and is likely related to the increase in winter temperature and rainfall after the Younger Dryas (cf. Litt *et al.* 2012; Cheddadi and Khater 2016; Roberts *et al.* 2018). The percentage of arboreal pollen starts decreasing gradually from 9500 to 6500 cal. yr. BP and seems not to be related to large-scale woodland clearance as the population decreases as well (Fig. 6). The pattern is also visible at a site-scale in the Southern Levant (Ein Gedi, Dead Sea, Sea of Galilee, Huleh) and in Northern Levant (Ammiq, Al Jourd; Fig. 7). Therefore, the drop of the AP assemblage could be linked to a period of increased aridity (cf. Litt *et al.* 2012). The shift from wetter climatic conditions that occurred for most of the PPNB to more arid conditions, exacerbated by the 8.2 ka event, could have stressed the Levantine social and economic system and negatively impacted upon the population, which seems to decrease significantly in the PNA (between ~8500 and 7500 cal. yr. BP) and stagnates for most of the PNB (see Fig. 2a-b and Fig. 3; cf. Bar-Yosef 2002; Kujit and Goring-Morris 2002; Flohr *et al.* 2016). Overall, the archaeological evidence suggests low population densities in southern and Lower North Levant during the Neolithic and the decrease of the AP assemblage seem difficult to relate to extensive farming and widespread land management (Rosen 2007, 99).

[Insert **Figure 7** about here]

5.2 Chalcolithic and Bronze Age (ca. 6450 – 3100 cal. yr. BP / 4500 – 1150 BCE)

Between the mid-seventh and the early sixth millennium cal. yr. BP a series of cultural changes and successful adaptations culminated in more complex societies throughout the Levant, which was characterised by a substantial increase of population and expansion of villages that in some cases reached an extent of ten hectares (Levy 1998; Rowan 2013; see Figs. 2-4). An overall increase in the number of settlements occur in all the four sub-regions (Fig. 3 and 4), and while most of the

sites are small in size, larger villages are known in the Lower Galilee (e.g. Beit Netofa, Horvat Usa, Tell Qiri), in the Cisjordan lowlands (e.g. Nazur, Meser) and in Northern Negev (e.g. Shiqmim, Abu Matar, Horvat Beter; cf. Levy *et al.* 2006; Rowan 2013). In this period, farming strategies became more intensive, with greater evidence for the production and consumption of cereals and newly domesticated olives (Galili *et al.* 1989 and 1997; Besnard *et al.* 2013), and of mixed livestock (but a prevalence of sheep and goat) that also became sources of secondary products such as milk and fibers (Levy 1992; Zohary *et al.* 2012). After 5800 cal. yr. BP population suffered a general decline and increased again during the EBA I, when the first proto-urban centres (measuring 10-30 ha) became common (Fig. 2 and 3). The Bronze Age is characterized by patterns of booms and busts where pronounced periods of population growth during the EBA I-III (~5300 – 4500 cal. yr. BP) and the MBA (~4000 – 3600 cal. yr. BP) were punctuated by a marked decline in population at the end of the IBA (~4200 – 4000 cal. yr. BP) and in the LBA (~3400 – 3200 cal. yr. BP) throughout the Levant (see Figs. 2-4; cf. Finkelstein 1993, 1994 and 1996; Finkelstein and Gophna 1993; Ofer 1994; Falconer and Savage 2009; Greenberg 2017). While the role of the 4.2 ka event in explaining population decrease is debated (cf. Weiss *et al.* 1993; Staubwasser and Weiss 2006; Rosen 2007; Kaniewski et al. 2008; Roberts et al. 2011; Finkelstein and Langgut 2014; Clarke et al. 2016), there is a broader consensus among scholars in recognizing the 3.2 ka event as having contributed to societal collapse (cf. Litt *et al.* 2012; Langgut *et al.* 2013; Kaniewski *et al.* 2008, 2010 and 2015; Izdebski *et al.*, 2016a). The impact of the 4.2 ka BP event is not easy to assess with the synthesised demographic proxies at 200-yr. resolution. The SPD of radiocarbon dates shows a significant decrease of population between 4200 cal. yr. BP and 4000 cal. yr. BP (Fig. 2a and 3), while the demographic trends described by the settlement data do not show a sharp decline in population that, instead, seem to stagnate across the IBA in the Southern Levant (Fig. 4b-d). This scenario could be the result of several factors such as the reduction of rainfall that would have hampered the creation of agricultural surplus, the lack of available marginal agro-pastoral areas given the successful expansion of walled settlements during the EBA II-III (~5000 – 4450 BP) and the exceeded carrying capacity of the land (Wilkinson *et al.* 2014, 90-92). It seems that a pronounced decline in population occurred in the Lower North Levant (Fig. 3a), where the demographic proxies are positively correlated with the drier climatic conditions depicted by the isotopic records from Jeita cave (Supplemental Material 2: Table S10).

The trend depicted by regional pastoral indicators seem to not corroborate the traditional view of the IBA as a period characterized by the spread of pastoral subsistence strategies (Horwitz 1989; Miroschedji 2009; Fig. 6). In fact, except the pollen record from Ein Gedi and Ammiq, the patterns showed by the other pollen sites do not show an increase of pastoral indicators (Fig. 8). Instead, the OJCV index from the Sea of Galilee, Birkat Ram and Ein Gedi (between 4200 – 4000 cal. yr. BP) indicate well-maintained orchards (Langgut *et al.* 2015; Fig. 7). All archaeological proxies show a substantial decrease in population in the LBA II-III (~3400 – 3200 cal. yr. BP; Figs 2 and 3). From the Chalcolithic onwards we observe a human-modified landscape as highlighted by a sharp increase of cultivated trees (OJCV: *Olea*, *Juglans*, *Castanea*, *Vitis*), which peaks in the EBA I at around 5500 cal. yr. BP (Fig. 6). A decrease of OJCV pollen values during the EBA II-III could be related to socio-economic causes rather than to climatic conditions as witnessed by the reduced demand of oil products from Egypt that established new trade relations with the communities in the North Levant (cf. Kaniewski *et al.* 2012; Langgut *et al.* 2014 and 2016). At a site-level scale this general trend is confirmed by all sites except Hula, which shows an increase of cultivated trees in the EBA II-III (~5000 – 4500 cal. yr. BP; Fig. 7). However, the OJCV pollen index is strongly related to the human activity and tends to vary according to the demographic dynamics (Table 3 and

Table S2). The proportion of arboreal pollen increased during the Chalcolithic and was steady across the whole Bronze Age indicating no particular evidence of human or climate impact (Fig. 6; Tables 3 and Supplemental Material 2: Table S1). The same pattern occurs at a site-level scale except for Ammiq and Al Jourd that reflect a stronger human activity such as oak and cedar deforestation (Fig. 7; Hajar *et al.* 2010). In this case, the secondary anthropogenic indicators (ruderal weeds + resistant grazing plants) from Al Jourd indicate an increase open fields and disturbed lands during the Chalcolithic and Bronze Age (~6500 – 3500 cal. yr. BP; Fig. 9). The API and the pastoral pollen indicators decrease during the Chalcolithic and the Bronze Age and are negatively correlated with demographic trends (Supplemental Material 2: Tables S3-S4) indicating that highly sedentary communities mostly rely on horticulture products rather than herd-based economy (Figs. 6 and 8). In fact, the EBA II-III (~5000 – 4450 BP) was characterized by the spreading of nucleated walled settlements in marginal agro-pastoral zones practising intensive agricultures and exerting the control over the surrounding lands and the agricultural products (cf. Philip 2003; Wilkinson et al. 2014, 88-90). An increase of the API and pastoral indicators occur in the LBA, in concomitance with a decline in population and cultivated trees (OJCV) and drier climatic conditions, perhaps indicating a shift in subsistence strategies of some local communities from intensive farming to pasture (Fig. 6 and 8). An increase of secondary anthropogenic indicators (ruderal weeds + grazing resistant plants) from 6500 BP onwards indicate a higher human impact on the natural environment (Fig. 6; Supplemental Material 2: Table S5) in the Cisjordan highlands (Ein Gedi), in the Huleh basin and on the Golan Heights (Birkat Ram; Fig.9).

[Insert **Figure 8** about here]

[Insert **Figure 9** about here]

5.3 From Iron Age I to the Persian period (ca. 3100 – 2283 cal. yr. BP / 1150 – 333 BCE)

The Iron Age is characterised by the decline of the Egyptian domination over the Southern Levant and by the establishment of medium-sized regional kingdoms such as Israel and Judah in the Southern Levant and Moab, Edom and Ammon in Transjordan, and Phoenician city-states in Lebanon and the northern coast of Israel. This is a period of highly complex societies and is characterised by the thriving of population in the IA I and II (~3100 – 2700 cal. yr. BP) particularly in Cisjordan and Transjordan (Fig. 2a-b and Fig. 3b-d). Although the SPD of radiocarbon dates may overestimate the population in this period given the possible research biases in collecting radiocarbon samples, this picture is corroborated by the trends described by the archaeological settlement data (Fig. 2b-c). However, studies on micro-regional scales show a reduction in human occupation at Akko and Tel Dan during phases of enduring drought (~3200-2700 cal. yr. BP) and a resurgence after 2500 cal. yr. BP, during the Persian and Hellenistic periods (cf. Kaniewski *et al.* 2013 and 2017). A decrease in population occurs in concomitance of the Persian domination (~ 2600 – 2300 cal. yr. BP) across the Southern Levant (Fig. 4b-d). During the Early Persian period (~2470 – 2400 cal. yr. BP) drier climatic conditions caused the abandonment of those steppe-marginal areas of the southern Levant, more fragile to climatic shifts, and prompted nomadization of some segments of the local population (cf. Langgut and Lipschits 2017).

During the Iron Age and Babylonian/Persian period, despite drier conditions indicated by the isotopic records from Soreq and Jeita caves, the overall trend is that population increased dramatically and was negatively correlated with palaeoclimate trends (Table 3 and Supplemental Material 2: S9-10). In fact, in this period, we may see a decoupling of demographic trends and

climate conditions because population is less vulnerable to climatic shifts due to advances in technologies coping with drought and food stress, and extensive trade networks and logistic infrastructures typical of state and empires, which are societies capable of transferring resources from areas with agricultural surplus to the ones with failed crops (Rosen 2007, 101; Wilkinson and Rayne 2010; Lawrence *et al.* 2016). Nevertheless, the patterns on micro-regional scale can depict a different scenario as local communities can experience different adaptation strategies to social and environmental stress. In the third millennium BP the parallelised gradual increase of OJCV, API, Simpson's Index, and pastoral indicators, and a decrease in AP percentage suggest that the landscape became heavily anthropogenised and that Levantine communities could have adopted a diversified subsistence economy as a response to climatic shifts (cf. Langgut *et al.* 2015; Finkelstein and Langgut 2018; Fig. 6).

5.4 Hellenistic, Roman and Byzantine Period (ca. 2282 – 1312 cal. yr. BP / 332 BCE – 638 AD)

Population started increasing in the latter half of the Hellenistic period and boomed throughout the Levant when the Roman Empire imposed its hegemony over the region (Bar 2004; Fig. 2b and 3). The population continued growing until the end of the Byzantine period (~1300 cal. yr. BP), when it reached the highest level ever, which was then reached again only in the twentieth century (Broshi 1979; Bar 2004; Scheidel 2007, 43). The Roman hegemony of the Mediterranean integrated the farming systems of the Levant into a large economic and political superstructure that mitigated the impact of climatic hazards and stimulated the production and management of highly demanded eastern Mediterranean products such as oil and wine (Alcock 2007). During this period the landscape was deeply transformed by human impact, reflecting the dramatic growth of population and a well-structured land management typical of imperial economies. The cultivated trees (OJCV) peaked across the Southern Levant (Fig. 6 and 7) and the olive-oil production occupied a very important role in the local economy as highlighted by the discovery of several heavy oil stone presses (cf. Safrai 1994; Ali 2014; Waliszewski 2014). The decrease of AP percentage (Figs. 5-6 and 7) and the simultaneous increase of API and pastoral indicators (Fig. 6 and 8) show the woodland clearance and the widespread of agriculture and an intensification of pasture. In particular, the very low percentage of AP at Chamsine and Aammiq reveal a heavy deforestation in favour of grazing activities (Hajar *et al.* 2010, 753-754; Fig. 7 and 8).

5.5 Early and Middle Islamic period (ca. 1312 – 458 cal. yr. BP / 638 – 1492 AD)

After the end of the Byzantine hegemony, the Levant was dominated by the Arabs, and the region was characterised by a decrease of population that slightly recovered between 1200 and 1500 cal. yr. BP without reaching the magnitude recorded during the Roman-Byzantine period. In the Early Islamic period, a sharp decline of cultivated trees (OJCV) accompanied by an increase of the evergreen shrubland (*Quercus*) is seen as evidence of forest regeneration and lowered human impact on the region (Figs. 5-6 and 7). A decrease in the API and pastoral indicators suggests that not only agriculture but also herd-based economy was affected by a general decline of population and the collapse of the Roman-Byzantine economic structures (Fig. 6). This trend occurred throughout the Levant and gradually slowed down in the Middle Islamic period (~1200 – 1500 cal. yr. BP) when population started increasing again (Fig. 8). The palaeoclimate records from Soreq and Jeita caves depict increased wetter conditions from ~1000 cal. yr. BP onwards, after dry conditions between 1300 and 1000 cal. yr. BP (Fig 6). The decrease of cultivated trees (OJCV) is not significantly correlated with climatic conditions (Supplemental Material 2: Table S7-8), while

shows a strong correlation with demographic proxies (Supplemental Material 2: Table S2). In fact, the decline of cultivation seems to slightly precede the climatic changes and is probably more related to the Arab conquest and the social and rural instability (Leroy 2010; Izdbeski *et al.* 2016, 204-205). In the end, the forest regeneration during the Islamic period could be the combination of decreased population and better climatic conditions.

6. Conclusions

This work has shown the socio-ecological trajectories occurring in the Levant across the Holocene. We adopted a multi-proxy and multi-scalar approach in order to assess if patterns of convergence and divergence between archaeological and environmental proxies (pollen and palaeoclimate records) vary at different geographical scales of analysis. The human footprint seems not to play a determinant role in the evolution of the Early Holocene landscape that, instead, seems to be more affected by abiotic factors. Despite a demographic increase after the onset of the Holocene, perhaps favoured by wetter climatic conditions, the population density was fairly low if compared with later periods and the Neolithic communities may have been more vulnerable to climatic shifts. In the Early Holocene, fluctuations in the percentage of arboreal pollen seems to be more related to climate change than to human activity. From the Chalcolithic onwards, the sharp increase of cultivated trees is positively correlated with demography, indicating more extensive farming to sustain a growing population. The Late Holocene landscape is heavily anthropogenised and characterised by a large-scale agricultural and herd-based economy that caused a pronounced woodland clearance during the Hellenistic-Roman-Byzantine period. The Late Holocene is also the period where the demographic trends appear to decouple from the climatic shifts given the advancements in technology and the extensive social and extensive networks of empires that geared the capability of local communities to deal with environmental stress. However, it is important to point out that in this study we defined some general trends on a broad chronological scale of analysis. In addition, it is difficult to disentangle the interplay of human and environmental dynamics with a 200-year resolution. In fact, marked climate fluctuations occurred within shorter time spans and so human populations would have immediately responded and progressively adapted to those changes over similar sub-centennial timescales. In addition, the regional scale of analysis adopted in this study does not allow us to discern localised socio-ecological trajectories. A future research endeavour will be of analysing human population and environmental dynamics at a micro-regional scale in order to assess how social behaviour varies in different ecological niches. Furthermore, a comparative approach on a broader geographical scale will be useful to assess how the socio-ecological dynamics occurring in the Levant are interrelated with the surrounding regions such as Egypt, Central Arabia and the Northern Fertile Crescent. It is clear from the present work that while a wealth of archaeological data exists in the Levant, a higher number of palaeoclimatic and pollen data are required to provide a more even spatial and chronological coverage and guarantee a more accurate interpretation. This could be possible with future tighter on-going interdisciplinary collaborations between archaeologists and natural scientists.

Acknowledgements

This work is the result of a workshop held in Mallorca in September 2017 under the umbrella of the Leverhulme Trust funded project "*Changing the Face of the Mediterranean: Land Cover and Population Since the Advent of Farming*" (Grant Ref. RPG-2015-031), a Plymouth-UCL collaboration. We are grateful to Steven Savage and Thomas Levy for allowing us to use a large portion of data from The Digital Archaeological Atlas of the Holy Land (DAAHL;

https://daahl.ucsd.edu/DAAHL/). Pollen data were extracted from the European Pollen Database (EPD; http://www.europeanpollendatabase.net/) and amalgamated from the work of data contributors. The EPD community is gratefully acknowledged and gratitude is given to Michelle Leydet (the EPD manager), and many data contributors who have made a valuable contribution to this research. We thank Alexander Kabelindde and Fayrouz Ibrahim for helping with the inputting and georeferencing of the radiocarbon dates. We are also grateful to Joan Estrany and the University of the Balearic Islands for hosting a workshop on Mallorca during which much of this work was discussed.

References

Alcock, S.E., 2007. The Eastern Mediterranean. In: Scheidel, W., Morris, I. and Saller, R.P. (Eds.), *The Cambridge economic history of the Greco-Roman world*. Cambridge: Cambridge University Press, 671-697.

Ali, N., 2014. Olive oil production in a semi-arid area: evidence from Roman Tell es-Sukhnah, Jordan. Mediterranean *Archaeology and Archaeometry 14*, 337-348.

Asouti, E. and Fuller, D.Q., 2012. From foraging to farming in the Southern Levant: The development of Epipalaeolithic and Pre-Pottery Neolithic plant management strategies. *Vegetation history and archaeobotany 21*(2), 149-162.

Asouti, E., Kabukcu, C., White, C.E., Kuijt, I., Finlayson, B. and Makarewicz, C., 2015. Early Holocene woodland vegetation and human impacts in the arid zone of the southern Levant. *The Holocene 25*(10), 1565-1580.

Bar, D., 2004. Population, settlement and economy in Late Roman and Byzantine Palestine (70–641 AD). *Bulletin of the School of Oriental and African Studies* 67(3), 307-320.

Bar-Matthews, M., Ayalon, A., Kaufman, A. and Wasserburg, G.J., 1999. The Eastern Mediterranean paleoclimate as a reflection of regional events: Soreq cave, Israel. *Earth and Planetary Science Letters* 166(1-2), 85-95.

Bar-Matthews, M., Ayalon, A., Gilmour, M., Matthews, A. and Hawkesworth, C.J., 2003. Sea–land oxygen isotopic relationships from planktonic foraminifera and speleothems in the Eastern Mediterranean region and their implication for paleorainfall during interglacial intervals. *Geochimica et Cosmochimica Acta 67*(17), 3181-3199.

Bar-Yosef, O., 2002. The Natufian culture and the early Neolithic: social and economic trends in southwestern Asia. In: P. Belwood and C. Renfrew (Eds.), *Examining the farming/language dispersal hypothesis*. Cambridge: University of Cambridge, 113-126.

Bar-Yosef, O., and Belfer-Cohen, A., 2002. Facing environmental crisis: Soci-etal and cultural changes at the transition from the Younger Dryasto the Holocene in the Levant. In: T. J. Cappers and S. Bottema (Eds.), *The Dawn of Farming in the Near East.* Berlin: Ex Oriente, 55–66.

Betts, A., 2013. The Southern Levant (Transjordan) During the Neolithic Period. . In: M. L. Steiner, and A. E. Killebrew (Eds.), *The Oxford Handbook of the Archaeology of the Levant: c. 8000-332 BCE*. Oxford: Oxford University Press, 171-182.

Bevan, A., Colledge, S., Fuller, D., Fyfe, R., Shennan, S. and Stevens, C., 2017. Holocene fluctuations in human population demonstrate repeated links to food production and climate. *Proceedings of the National Academy of Sciences*, p.201709190.

Besnard, G., Khadari, B., Navascués, M., Fernández-Mazuecos, M., El Bakkali, A., Arrigo, N., Baali-Cherif, D., de Caraffa, V.B.B., Santoni, S., Vargas, P. and Savolainen, V., 2013. The complex history of the olive tree: from Late Quaternary diversification of Mediterranean lineages to primary domestication in the northern Levant. *Proceedings of the Royal Society B 280*(1756), p.20122833.

Bienert, H. D., 2004. The Pre-Pottery Neolithic B (PPNB) in Jordan: first steps towards proto-urban societies? In: H.-D. Bienert, H.-G. K. Gebel, and R. Neef (Eds.), *Central Settlements in Neolithic Jordan: Proceedings of a Symposium Held in Wadi Musa, Jordan, 21st–25th of July, 1997*. Berlin: Ex oriente, 21–40.

Borrell, F., Junno, A., Barcel_o, J.A., 2015. Synchronous environmental and cultural change in the emergence of agricultural economies 10,000 Years ago in the Levant. *PLoS ONE* 10 (8), e0134810. https://doi.org/10.1371/journal.pone.0134810

Braun E. 2012. On some south Levantine Early Bronze Age ceramic “wares” and styles. *Palestine Exploration Fund Quarterly 144*, 4–31.

Broshi, M., 1979. The population of western Palestine in the Roman-Byzantine period. *Bulletin of the American Schools of Oriental Research* 236, 1-10.

Butlin, R.A., and Roberts, N. (eds.), 1995. *Ecological relations in historical times: human impact and adaptation*. Oxford: Blackwell.

Cheddadi, R. and Khater, C., 2016. Climate change since the last glacial period in Lebanon and the persistence of Mediterranean species. *Quaternary Science Reviews 150*, 146-157.

Cheng, H., Sinha, A., Verheyden, S., Nader, F.H., Li, X.L., Zhang, P.Z., Yin, J.J., Yi, L., Peng, Y.B., Rao, Z.G. and Ning, Y.F., 2015. The climate variability in northern Levant over the past 20,000 years. *Geophysical Research Letters 42*(20), 8641-8650.

Clarke, J., Brooks, N., Banning, E.B., Bar-Matthews, M., Campbell, S., Clare, L., Cremaschi, M., di Lernia, S., Drake, N., Gallinaro, M. and Manning, S., 2016. Climatic changes and social transformations in the Near East and North Africa during the ‘long’4th millennium BC: A comparative study of environmental and archaeological evidence. *Quaternary Science Reviews 136*, 96-121.

Colledge, S.M., 1998. Identifying Pre-domestication Cultivation Using Multivariate Analysis. In: A. B. Damania, J. Valkoun, G. Willcox, and C. O. Qualset (Eds.), *The Origins of Agriculture and Crop Domestication*. Rome: International Plant Genetic Resources Institute, 121-131.

Colledge, S., Conolly, J., Shennan, S., Bellwood, P., Bouby, L., Hansen, J., Harris, D., Kotsakis, K., zdoan, M., Peltenburg, E. and Willcox, G., 2004. Archaeobotanical evidence for the spread of farming in the Eastern Mediterranean. *Current anthropology* 45(S4), 35-58.

Cordova, C., 2007. *Millennial Landscape Change in Jordan: Geoarchaeology and Cultural Ecology*. Tucson: University of Arizona Press.

Crema, E.R., 2012. Modelling temporal uncertainty in archaeological analysis. *Journal of Archaeological Method and Theory 19(3)*, 440-461.

Crema, E.R., and Bevan, A., 2018. rcarbon v1.1.2 : Methods for calibrating and analysing radiocarbon dates URL: https://CRAN.R-project.org/package=rcarbon

Crema, E. R., Bevan, A., and Lake, M., 2010. A probabilistic framework for assessing spatio-temporal point patterns in the archaeological record. *Journal of Archaeological Science 37*, 1118–1130.

Crema, E.R., Habu, J., Kobayashi, K. and Madella, M., 2016. Summed Probability Distribution of 14 C Dates Suggests Regional Divergences in the Population Dynamics of the Jomon Period in Eastern Japan. *PloS one 11*(4), p.e0154809.

Danin, A., 1988. Flora and vegetation of Israel and adjacent areas. In: Y. Yom Tov, and E. Tchernov (Eds.), *The zoogeography of Israel*. Dordrecht: Junk Publishers, 129–159.

Davis BAS, Zanon M, Collins P, et al. (2013) The European modern pollen database (EMPD) project. Vegetation History and Archaeobotany 22: 521-530.

Djamali, M., Akhani, H., Andrieu-Ponel, V., Braconnot, P., Brewer, S., de Beaulieu, J.-L., Fleitmann, D., Fleury, J., Gasse, F., Guibal, F., Jackson, S.T., Lézine, A.-M., Médail, F., Ponel, F., Roberts, N., Stevens, L., 2010. Indian Summer Monsoon variations could have affected the early Holocene woodland expansion in the Near East. *Holocene* 20, 813-820.

Drennan, R.D., Berrey, C.A. and C. E., Peterson, 2015. *Regional Settlement Demography in Archaeology*. New York: Eliot Werner Publications.

Eastwood, W. J., Roberts, N., and Lamb H. F., 1998. Palaeoecological and archaeological evidence for human occupance in southwest Turkey: The Beyşehir Occupation Phase. *Anatolian Studies 48*, 69-86.

Enzel, Y. and Bar-Yosef, O. Eds., 2017. *Quaternary of the Levant: Environments, Climate Change, and Humans*. Cambridge: Cambridge University Press.

Falconer, S.E. and Savage, S.H., 2009. The Bronze Age political landscape of the Southern Levant. In: S. E. Falconer and C. L. Redman (Eds.), *Polities and Power: Archaeological Perspectives on the Landscapes of Early States.* Tucson: University of Arizona Press, 125-151.

Fall, P.L., Soto-Berelov, M., Ridder, E. and, Falconer, S.E., 2018. Toward a Grand Narrative of Bronze Age Vegetation Change and Social Dynamics in the Southern Levant. In: T.E. Levy and I. Jones (Eds.) *Cyber-Archaeology and Grand Narratives: Digital Technology and Deep-Time Perspectives on Culture Change in the Middle East*. New York: Springer, 91-110.

Finkelstein, I., 1993. Environmental Archaeology and Social History: Demographic and Economic Aspects of the Monarchic Period. In: A. Biran J. Aviram, and A. Paris-Shadur (Eds.), *Biblical Archaeology Today, 1990: Proceedings of the Second International Congress on Biblical Archaeology.* Jerusalem: Israel Exploration Society, 56-66.

Finkelstein, I., 1994. The Emergence of Israel: A Phase in the Cyclic history of Canaan in the Third and Second millennia BCE. In: I. Finkelsten, and N. Na'aman (Eds.), *From Nomadism to Monarchy: Archaeological and Historical Aspects of Early Israel*. Jerusalem: Israel Exploration Society, 150-178.

Finkelstein, I., 1995. The great transformation: The 'conquest' of the highlands frontiers and the rise of the territorial states. In: T. E. Levy (Ed.), *The Archaeology of Society in the Holy Land*. Leicester: University Press, 349–365.
Finkelstein, I., 1996. Ethnicity and origin of the Iron I settlers in the highlands of Canaan: can the real Israel stand up?. *The Biblical Archaeologist* 59(4), 198-212.

Finkelstein, I. 1998. The Rise of Early Israel Archaeology and Long-Term History. In: A. Shmuel and E. D. Oren (Eds.), *The Origin of Early Israel, current debate*. Jerusalem: Posner & Sons Ltd, 7-39.

Finkelstein, I., 2013. *The Forgotten Kingdom. The Archaeology and History of Northern Israel.* Atlanta: Society of Biblical Literature.

Finkelstein, I. and Gophna, R. 1993. Settlement, demographic, and economic patterns in the highlands of Palestine in the Chalcolithic and Early Bronze periods and the beginning of urbanism. *Bulletin of the American Schools of Oriental Research 289*, 1–22.

Finkelstein, I. and Langgut, D., 2014. Dry climate in the Middle Bronze I and its impact on settlement patterns in the Levant and beyond: new pollen evidence. *Journal of Near Eastern Studies 73*(2), 219-234.

Finkelstein, I., and Langgut, D., 2018. Climate, Settlement History, and Olive Cultivation in the Iron Age Southern Levant. *Bulletin of the American Schools of Oriental Research* 379, 153-169.

Finkelstein, I. and Piasetzky, E., 2010. The Iron I/IIA transition in the Levant: a reply to Mazar and Bronk Ramsey and a new perspective. *Radiocarbon 52*(4), 1667-1680.

Finkelstein, I. and Piasetzky, E., 2011. The Iron Age chronology debate: Is the gap narrowing? *Near Eastern Archaeology 74*(1), 50-54.

Finlayson, B., and Warren, G., 2010. *Changing natures: hunter-gatherers, first farmers, and the modern world*. Duckworth: London.

Finlayson, B., 2013. Introduction to the Levant During the Neolithic Period. In: M. L. Steiner, and A. E. Killebrew (Eds.), *The Oxford Handbook of the Archaeology of the Levant: c. 8000-332 BCE*. Oxford: Oxford University Press, 124-133.

Fyfe RM, Woodbridge, J. and Roberts N., 2018. Trajectories of change in Mediterranean Holocene vegetation through classification of pollen data. *Vegetation History and Archaeobotany* 27: 351-364.

Galili, E., Weinstein-Evron, M., and Zohary, D., 1989. Appearance of olives in submerged Neolithic sites along the Carmel coast. *Journal of the Israel Prehistoric Society 22*, 95-97.

Galili, E., Stanley, D.J., Sharvit, J. and Weinstein-Evron, M., 1997. Evidence for earliest olive-oil production in submerged settlements off the Carmel coast, Israel. *Journal of Archaeological Science 24*(12), 1141-1150.

Geva, H., 2014. Jerusalem's population in antiquity: a minimalist view. *Tel Aviv 41*(2), 131-160.

Giesecke, T., Davis, B., Brewer, S., Finsinger, W., Wolters, S., Blaauw, M., De Beaulieu, J.L., Binney, H., Fyfe, R.M., Gaillard, M.J. and Gil-Romera, G., 2014. Towards mapping the late Quaternary vegetation change of Europe. *Vegetation History and Archaeobotany 23*(1), 75-86.

Greenberg, R., 2002. *Early Urbanizations in the Levant: A Regional Narrative*. London: Leicester University Press.

Greenberg, R., 2017. No collapse: transmutations of Early Bronze Age urbanism in the Southern Levant. In: F. Höflmayer (Ed.), *The Late Third Millennium in the Ancient Near East: Chronology, C14 and Climate Change; Papers from the Oriental Institute Seminar Held at the Oriental Institute of the University of Chicago, 7–8 March 2014*. Chicago: Oriental Institute of the University of Chicago, 33-60.

Greenberg, R. and Keinan, A., 2009. *Israeli archaeological activity in the West Bank 1967-2007: A sourcebook*. Jerusalem: Ostracon.

Gophna, R. and Portugali, J., 1988. Settlement and demographic processes in Israel's coastal plain from the Chalcolithic to the Middle Bronze Age. *Bulletin of the American Schools of Oriental Research* 269, 11-28.

Goring-Morris, A.N., Belfer-Cohen, A., 2008. A roof over one's head: developments in Near Eastern residential architecture across the EpipalaeolithiceNeolithic transition. In: Boquet-Appel, J.P., Bar-Yosef, O. (Eds.), *The Neolithic Demographic Transition and its Consequences*. Dordrecht: Springer Netherlands, 239-286.

Goring-Morris, A.N. and Belfer-Cohen, A., 2010. 'Great expectations', or, the inevitable collapse of the Early Neolithic in the Near East. In: M. S. Bandy and J. R. Fox (Eds.), *Becoming Villagers: Comparing Early Village Societies*. Tucson: University of Arizona Press, 62–77.

Goring-Morris, A.N. and Belfer-Cohen, A., 2013. The Southern Levant (Cisjordan) during the Neolithic period. In: M. L. Steiner, and A. E. Killebrew (Eds.), *The Oxford Handbook of the Archaeology of the Levant: c. 8000-332 BCE*. Oxford: Oxford University Press, 148 – 169.

Hajar, L., Khater, C. and Cheddadi, R., 2008. Vegetation changes during the late Pleistocene and Holocene in Lebanon: a pollen record from the Bekaa Valley. *The Holocene 18*(7), 1089-1099.

Hajar, L., Haïdar-Boustani, M., Khater, C. and Cheddadi, R., 2010. Environmental changes in Lebanon during the Holocene: Man vs. climate impacts. *Journal of Arid Environments* 74(7), 746-755.

Horwitz, L.K., 1989. Sedentism in the Early Bronze IV: a faunal perspective. Bulletin of the American Schools of Oriental Research, pp.15-25.

Horwitz, L. K., E. Tchernov, P. Ducos, et al. (2000). Animal domestication in the southern Levant. Paléorient 25, 63–80.

Issar, A. S., and Zohar, M., 2004. *Climate Change: Environment and Civilization in the Middle East.* Berlin: Springer.

Izdebski, A., Pickett, J., Roberts, N. and Waliszewski, T., 2016a. The environmental, archaeological and historical evidence for regional climatic changes and their societal impacts in the Eastern Mediterranean in Late Antiquity. *Quaternary Science Reviews* 136, 189-208.

Izdebski, A., Holmgren, K., Weiberg, E., Stocker, S.R., Büntgen, U., Florenzano, A., Gogou, A., Leroy, S.A., Luterbacher, J., Martrat, B. and Masi, A., 2016b. Realising consilience: How better communication between archaeologists, historians and natural scientists can transform the study of past climate change in the Mediterranean. *Quaternary Science Reviews 136*, 5-22.

Kadosh, D., Sivan, D., Kutiel, H. and Weinstein-Evron, M., 2004. A late quaternary paleoenvironmental sequence from Dor, Carmel coastal plain, Israel. *Palynology 28*(1), 143-157.

Kaniewski, D., Paulissen, E., Van Campo, E., Al-Maqdissi, M., Bretschneider, J. and Van Lerberghe, K., 2008. Middle East coastal ecosystem response to middle-to-late Holocene abrupt climate changes. *Proceedings of the National Academy of Sciences* 105(37), 13941-13946.

Kaniewski, D., Paulissen, E., Van Campo, E., Weiss, H., Otto, T., Bretschneider, J. and Van Lerberghe, K., 2010. Late second–early first millennium BC abrupt climate changes in coastal Syria and their possible significance for the history of the Eastern Mediterranean. *Quaternary Research 74*(2), 207-215.

Kaniewski, D., Van Campo, E., Boiy, T., Terral, J.F., Khadari, B., and Besnard, G., 2012. Primary domestication and early uses of the emblematic olive tree: palaeobotanical, historical and molecular evidence from the Middle East. *Biological Reviews 87*(4), 885-899.

Kaniewski, D., Van Campo, E., Morhange, C., Guiot, J., Zviely, D., Shaked, I., Otto, T. and Artzy, M., 2013. Early urban impact on Mediterranean coastal environments. *Scientific reports* 3, 3540.

Kaniewski, D., Van Campo, E., Morhange, C., Guiot, J., Zviely, D., Le Burel, S., Otto, T. and Artzy, M., 2014. Vulnerability of Mediterranean ecosystems to long-term changes along the coast of Israel. *PloS one 9*(7), p.e102090.

Kaniewski, D., Guiot, J. and Van Campo, E., 2015. Drought and societal collapse 3200 years ago in the Eastern Mediterranean: a review. *Wiley Interdisciplinary Reviews: Climate Change 6* (4), 369-382.

Kaniewski, D., Marriner, N., Ilan, D., Morhange, C., Thareani, Y. and Van Campo, E., 2017. Climate change and water management in the biblical city of Dan. *Science advances 3*(11), p.e1700954.

Kolář, J., Macek, M., Tkáč, P. and Szabó, P., 2016. Spatio-Temporal Modelling As A Way to Reconstruct Patterns of Past Human Activities. *Archaeometry 58*(3), 513-528.

Kuijt, I. and Goring-Morris, N., 2002. Foraging, farming, and social complexity in the Pre-Pottery Neolithic of the Southern Levant: a review and synthesis. *Journal of World Prehistory* 16 (4), 361-440.

Langgut, D., 2018. Late Quaternary Nile flows as recorded in the Levantine Basin: The palynological evidence. *Quaternary International 464*, 273-284.

Langgut, D., Almogi-Labin, A., Bar-Matthews, M. and Weinstein-Evron, M., 2011. Vegetation and climate changes in the South Eastern Mediterranean during the Last Glacial-Interglacial cycle (86 ka): new marine pollen record. *Quaternary Science Reviews 30*(27-28), 3960-3972.

Langgut, D., Finkelstein, I. and Litt, T. 2013. Climate and the Late Bronze collapse: new evidence from the Southern Levant. *Tel Aviv* 40, 149–75.

Langgut, D., Neumann, F. H., Stein, M., Wagner, A., Kagan, E. J., Boaretto, E. and Finkelstein, I. 2014. Dead Sea pollen record and history of human activity in the Judean Highlands (Israel) from the Intermediate Bronze into the Iron Ages (~2500–500 BCE). *Palynology* 38, 280–302.

Langgut, D., Finkelstein, I., Litt, T., Neumann, H. F. and Stein, M. 2015. Vegetation and climate changes during the Bronze and Iron Ages (~3600–600 BCE) in the Southern Levant based on palynological records. *Radiocarbon* 57, 217–35.

Langgut, D., Adams, M.J. and Finkelstein, I., 2016. Climate, settlement patterns and olive horticulture in the Southern Levant during the Early Bronze and Intermediate Bronze Ages (c. 3600–1950 BC). *Levant* 48(2), 117-134.

Langgut, D., and Lipschits, O., 2017. Dry Climate during the Babylonian and the Early Persian Period and its Impact on the Creation of Idumea. *Transeuphraténe 49*, 141-172.

Lawrence, D., Philip, G., Hunt, H., Snape-Kennedy, L. and Wilkinson, T.J., 2016. Long term population, city size and climate trends in the Fertile Crescent: A first approximation. *PloS one 11*(3), p.e0152563.

Leroy, S.A., 2006. From natural hazard to environmental catastrophe: Past and present. *Quaternary International 158*(1), 4-12.

Leroy, S.A., 2010. Pollen analysis of core DS7-1SC (Dead Sea) showing intertwined effects of climatic change and human activities in the Late Holocene. *Journal of Archaeological Science 37*(2), 306-316.

Leroy, S. A., 2018. Pollen profile DS7, Dead Sea. European Pollen Database (EPD), PANGAEA, https://doi.pangaea.de/10.1594/PANGAEA.889367
Leroy, S.A., Marco, S., Bookman, R. and Miller, C.S., 2010. Impact of earthquakes on agriculture during the Roman–Byzantine period from pollen records of the Dead Sea laminated sediment. *Quaternary Research 73*(2), 191-200.

Levy, T. E., 1992. Transhumance, Subsistence, and Social Evolution. In: O. Bar-Yosef and A. M. Khazanov (Eds.), *Pastoralism in the Levant: Archaeological Materials in Anthropological Perspectives.* Madison, WI: Prehistory Press, 65-82.

Levy, T. E., 1998. Cult, Metallurgy and Rank Societies: Chalcolithic Period (ca. 4500 – 3500 BCE). In: T. E. Levy (Ed.), *The Archaeology of Society in the Holy Land.* London: Leicester University Press, 227-244.

Levy, T.E., Burton, M., Rowan, Y. M., 2006. Chalcolithic hamlet excavations near Shiqmim, Negev Desert, Israel. *Journal of Field Archaeology 31*, 41–60.

Leydet M. 2007-2017. The European Pollen Database. Available at: http://www.europeanpollendatabase.net/. (accessed October 2017).

Litt, T., Ohlwein, C., Neumann, F.H., Hense, A. and Stein, M., 2012. Holocene climate variability in the Levant from the Dead Sea pollen record. *Quaternary Science Reviews 49*, 95-105.

Maher, L.A., Banning, E.B., Chazan, M., 2011. Oasis or Mirage? Assessing the role ofabrupt climate change in the prehistory of the southern levant. *Cambridge Archaeological Journal* 21(1), 1-30.

Mazar, A., and Bronk Ramsey, C., 2008. 14C dates and the Iron Age chronology of Israel: a response. *Radiocarbon 50*(2), 159–80.

Mazar, A., and Bronk Ramsey, C., 2010. A Response to Finkelstein and Piasetzky's Criticism and "New Perspective." *Radiocarbon 52*, 1681–88.

Mazier F, Galop D, Brun C, et al., 2006. Modern pollen assemblages from grazed vegetation in the western Pyrenees, France: a numerical tool for more precise reconstruction of past cultural landscapes. The Holocene 16: 91-103.

Mazier, F., Galop, D., Gaillard, M.-J, Rendu, C., Cugny, C., Legaz, A., Peyron, O., Buttler, A., 2009. Multidisciplinary approach to reconstruct pastoral activities. An example from the PyreneanMountains (Pays Basque). *Holocene 19*, 171–178

Mercuri AM, Bandini Mazzanti M, Florenzano A, et al., 2013a. Anthropogenic pollen indicators (API) from archaeological sites as local evidence of human-induced environments in the Italian Peninsula. Annali Di Botanica 3, 143-153.

Mercuri AM, Bandini Mazzanti M, Florenzano A, et al., 2013b. Olea, Juglans and Castanea: The OJC group as pollen evidence of the development of human-induced environments in the Italian peninsula. Quaternary International 303. 24-42.

Michczyńska, D.J., Pazdur, A., 2004. Shape analysis of cumulative probability density function of radiocarbon dates set in the study of climate change in late glacial and holocene. *Radiocarbon* 46 (2), 733 – 744.

Michczyńska, D.J., Michczyński, A., Pazdur, A., 2007. Frequency distribution of radiocarbon dates as a tool for reconstructing environmental changes. *Radiocarbon* 49 (2), 799 – 806.

Miroschedji, P.D., 2009. Rise and collapse in the Southern Levant in the Early Bronze Age. *Scienze dell'antichità 15*, 101-129.

Morris, E.K., Caruso, T., Buscot, F., Fischer, M., Hancock, C., Maier, T.S., Meiners, T., Müller, C., Obermaier, E., Prati, D. and Socher, S.A., 2014. Choosing and using diversity indices: insights for ecological applications from the German Biodiversity Exploratories. *Ecology and evolution 4(*18*)*, 3514-3524.

Neumann, F.H., Kagan, E.J., Schwab, M.J. and Stein, M., 2007. Palynology, sedimentology and palaeoecology of the late Holocene Dead Sea. *Quaternary Science Reviews 26*(11-12), 1476-1498.

Ofer, A., 1994. 'All the hill country of Judah': from settlement fringe to a prosperous monarchy. In, Finkelstein, I. and Na'aman, N. (Eds.), *From Nomadism to Monarchy: Archaeolgoical and Historical Aspects of Early Israel*. Jerusalem: Israel Exploration Society, 92–121.

Orton, D., Morris, J. and Pipe, A., 2017. Catch Per Unit Research Effort: Sampling Intensity, Chronological Uncertainty, and the Onset of Marine Fish Consumption in Historic London. *Open Quaternary 3*(1), 1-20.

Palmisano, A., Bevan, A. and Shennan, S., 2017. Comparing archaeological proxies for long-term population patterns: An example from central Italy. *Journal of Archaeological Science 87*, 59-72.

Philip, G., 2003. The Early Bronze Age of the southern Levant: a landscape approach. *Journal of Mediterranean Archaeology 16*(1), 103-132.

Philip, G., 2011. The later prehistory of the Southern Levant: issues of practice and context. In: Rowan, Y.M., and Lovell, J.L. (Eds.), *Culture, Chronology and the Chalcolithic: Theory and Transition.* Levant Supplementary Series 9. Oxford: CBRL Monographs, 189-206.

Porter, B.W., 2016. Assembling the Iron Age Levant: The Archaeology of Communities, Polities, and Imperial Peripheries. *Journal of Archaeological Research 24*(4), 373-420.

Rambeau, C.M., 2010. Palaeoenvironmental reconstruction in the Southern Levant: synthesis, challenges, recent developments and perspectives. *Philosophical Transactions of the Royal Society of London A: Mathematical, Physical and Engineering Sciences 368*(1931), 5225-5248.

Regev, J., De Miroschedji, P., Greenberg, R., Braun, E., Greenhut, Z. and Boaretto, E., 2012. Chronology of the Early Bronze Age in the Southern Levant: new analysis for a high chronology. *Radiocarbon 54*(3-4), 525-566.

Reimer, P.J., Bard, E., Bayliss, A., Beck, J.W., Blackwell, P. G., Bronk-Ramsey, C., et al., 2013. IntCal13 and Marine13 radiocarbon age calibration curves 0–50,000 Years cal BP. *Radiocarbon 55*(4), 1869–1887.

Roberts, N., Eastwood, W.J., Kuzucuoğlu, C., Fiorentino, G. and Caracuta, V., 2011. Climatic, vegetation and cultural change in the eastern Mediterranean during the mid-Holocene environmental transition. *The Holocene* 21(1), 147-162.

Roberts, N., Woodbridge, J., Bevan, A., Palmisano, A., Shennan, S., and Asouti, E., 2018. Human responses and non-responses to climatic variations during the last glacial-interglacial transition in the eastern Mediterranean. *Quaternary Science Reviews* 184, 47-67.

Roberts, N., Woodbridge, J., Palmisano, A., Bevan, A., Fyfe, R., and Shennan, S. Mediterranean landscape change during the Holocene: synthesis, comparison and regional trends in population, land cover and climate. *The Holocene.*

Rollefson, G. O., 2001. The Neolithic period. In: B. MacDonald, R. Adams, and P. Bienkowski (Eds.), *The Archaeology of Jordan*. Sheffield: Sheffield Academic, 67–105.

Rosen, A.M., 2007. *Civilizing climate: social responses to climate change in the ancient Near East*. Lanham, MD: Altamira Press.

Rosen, A. M., and Rosen, S. A., 2017. Environmental Change and Society in Holocene Prehistory. In: Y. Enzel and O. Bar-Yosef (Eds.), *Quaternary of the Levant: Environments, Climate Change and Humans.* Cambridge: Cambridge University Press, 1405-1422.

Rowan, Y. M., 2013. The Southern Levant (Cisjordan) During the Chalcolithic Period. In: M. L. Steiner, and A. E. Killebrew (Eds.), *The Oxford Handbook of the Archaeology of the Levant: c. 8000-332 BCE*. Oxford: Oxford University Press, 224-236.

Safrai, Z.E., 2003. *The economy of roman Palestine*. Routledge.

Savage, S. H, Falconer, S. E., and Harrison, T., 2007. The Early Bronze Age City States of Southern Levant. Neither Cities nor States. In: T. E. Levy, P. M. Michèle Daviau, R. W. Younker, and M. Shaer (Eds.), *Crossing Jordan: North American Contributions to the Archaeology of Jordan*. London: Equinox, 285–97.

Savage, S.H. and Levy, T.E., 2014. DAAHL—The digital archaeological atlas of the holy land: A model for Mediterranean and world archaeology. *Near Eastern Archaeology 77*(3), 243-247.

Scheidel, W., 2007. *Demography*. In: Scheidel, W., Morris, I. and Saller, R.P. (Eds.), *The Cambridge economic history of the Greco-Roman world* . Cambridge: Cambridge University Press, 38-86.

Schiebel, V. and Litt, T., 2017. Holocene vegetation history of the Southern Levant based on a pollen record from Lake Kinneret (Sea of Galilee), Israel. *Vegetation History and Archaeobotany*. https://doi.org/10.1007/s00334-017-0658-3

Schwab, M.J., Neumann, F., Litt, T., Negendank, J.F. and Stein, M., 2004. Holocene palaeoecology of the Golan Heights (Near East): investigation of lacustrine sediments from Birkat Ram crater lake. *Quaternary Science Reviews* 23, 1723-1731.

Sharon, I., 2013. Levantine chronology. In: M. L. Steiner, and A. E. Killebrew (Eds.), *The Oxford Handbook of the Archaeology of the Levant: c. 8000-332 BCE*. Oxford: Oxford University Press, 44-65.

Staubwasser, M. and Weiss, H., 2006. Holocene climate and cultural evolution in late prehistoric–early historic West Asia. *Quaternary Research 66*(3), 372-387.

Stein, M., Torfstein, A., Gavrieli, I., Yechieli, Y., 2010. Abrupt aridities and salt deposition in the post-glacial Dead Sea and their North Atlantic connection. *Quaternary Science Reviews 29*, 567-575.

Suriano, M., 2013. Historical geography of the ancient Levant. In: M. L. Steiner, and A. E. Killebrew (Eds.), *The Oxford Handbook of the Archaeology of the Levant: c. 8000-332 BCE*. Oxford: Oxford University Press, 9-23.

Timpson, A., Colledge, S., Crema, E., Edinborough, K., Kerig, T., Manning, K., Thomas, M.G. and Shennan, S., 2014. Reconstructing regional population fluctuations in the European Neolithic using radiocarbon dates: a new case-study using an improved method. *Journal of Archaeological Science 52*, 549-557.

Turchin, P. 2001. Does population ecology have general laws? *Oikos 94* (1), 17-26.

van Zeist, W. and Bottema, S. 1991. *Late Quaternary Vegetation of the Near East*. Wiesbaden: Dr Ludwig Reichert Verlag.

van Zeist, W., Baruch, U. and Bottema, S., 2009. Holocene palaeoecology of the Hula area, northeastern Israel. In: E. Kaptijn and L. P. Petit (Eds.), *A Timeless Vale. Archaeological and Related Essays on the Jordan Valley in Honour of Gerrit Van Der Kooij on the Occasion of his Sixty-Fifth Birthday*. Leiden: Leiden University Press, 29-64.

Vrydaghs, L., and T. Denham (2007). Rethinking agriculture: introductory thoughts. In: T. Denham, J. Iriarte, and L. Vrydaghs (Eds.), *Rethinking Agriculture: Archaeological and Ethnoarchaeological Perspectives*. Walnut Creek: Left Coast Press, 1–15.

Waliszewski, T., 2014. *Elaion: Olive Oil Production in Roman and Byzantine Syria-Palestine*. Warsaw: University of Warsaw Press.

Weiss, H., Courty, M.A., Wetterstrom, W., Guichard, F., Senior, L., Meadow, R. and Curnow, A., 1993. The genesis and collapse of third millennium north Mesopotamian civilization. *Science 261*(5124), 995-1004.

Weninger, B., Clare, L., Rohling, E., Bar-Yosef, O., Böhner, U., Budja, M., Bundschuh, M., Feurdean, A., Gebe, H.G., Jöris, O. and Linstädter, J., 2009. The impact of rapid climate change on

prehistoric societies during the Holocene in the Eastern Mediterranean. *Documenta praehistorica 36*, 7-59.

Weninger, B., Clare, L., Jöris, O., Jung, R. and Edinborough, K., 2015. Quantum theory of radiocarbon calibration. *World Archaeology 47*(4), 543-566.

Williams, A.N., 2012. The use of summed radiocarbon probability distributions in archaeology: a review of methods. *Journal of Archaeological Science* 39(3), 578-589.

Wilkinson, T. J., and Rayne, L., 2010. Hydraulic landscapes and imperial power in the Near East. *Water History 2*(2), 115-144.

Wilkinson, T.J., Philip, G., Bradbury, J., Dunford, R., Donoghue, D., Galiatsatos, N., Lawrence, D., Ricci, A. and Smith, S.L., 2014. Contextualizing early urbanization: Settlement cores, early states and agro-pastoral strategies in the Fertile Crescent during the fourth and third millennia BC. *Journal of World Prehistory 27*(1), 43-109.

Woodbridge, J., Roberts, N. and Fyfe, R., 2018. Pan-Mediterranean Holocene vegetation and land-cover dynamics from synthesised pollen data. *Journal of Biogeography 45* (9), 2159-2174.

Lu, Y., Waldmann, N., Nadel, D. and Marco, S., 2017. Increased sedimentation following the Neolithic Revolution in the Southern Levant. *Global and Planetary Change 152*, 199-208.

Ziv, B., Dayan, U., Kushnir, Y., Roth, C. and Enzel, Y. 2006. Regional and global atmospheric patterns governing rainfall in the Southern Levant. *International Journal of Climatology* 26, 55–73.

Zohary, M., 1962. *Plant life of Palestine*. New York: Ronald Press Co.

Zohary, M., 1973. *Geobotanical Foundations of the Middle East*. Stuttgart: Fischer.

Zohary, D., Hopf, M. and Weiss, E., 2012. *Domestication of Plants in the Old World: The origin and spread of domesticated plants in Southwest Asia, Europe, and the Mediterranean Basin*. Oxford: Oxford University Press.

Period	Absolute dates	
Pre-Pottery Neolithic A (PPNA)	9800 – 8700/8500 BCE	11750 – 10650/10450 BP
Pre-Pottery Neolithic B (PPNB)	8700/8500 – 6400 BCE	10650/10450 – 8350 BP
Pottery Neolithic A/Late Neolithic 1	6400 – 5500 BCE	8350 – 7450 BP
Pottery Neolithic B/Late Neolithic 2	5500 – 4500 BCE	7450 – 6450 BP
Chalcolithic	4500 – 3800/3600 BCE	6450 – 5750/5550 BP
Early Bronze Age IA	3800/3600 – 3300 BCE	5750/5550 – 5250 BP
Early Bronze Age IB	3300 – 3050/3000 BCE	5250 – 5000/4950 BP
Early Bronze Age II	3050/3000 – 2850/2800 BCE	5000/4950 – 4800/4750 BP
Early Bronze Age III	2850/2800 – 2500 BCE	4800/4750 – 4450 BP
Intermediate Bronze Age/Early Bronze Age IV	2500 – 2000/1950 BCE	4450 – 3950/3900 BP
Middle Bronze Age I	2000/1950 – 1750 BCE	3950/3900 – 3700 BP
Middle Bronze Age II-III	1750 – 1550 BCE	3700 – 3500 BP
Late Bronze Age I	1550 -1400 BCE	3500 – 3350 BP
Late Bronze Age II	1400 – 1200 BCE	3350 – 3150 BP
Late Bronze Age III	1200 – 1150 BCE	3150 – 3100 BP
Iron Age I	1150 – 950 BCE	3100 – 2900 BP
Iron Age IIA	950 – 780 BCE	2900 – 2730 BP
Iron Age IIB	780 – 680 BCE	2730 – 2630 BP
Iron Age IIC	680 – 586 BCE	2630 – 2536 BP
Babylonian	586 – 539 BCE	2536 – 2489 BP
Persian	539 – 333 BCE	2489 – 2283 BP
Hellenistic	332 – 63 BCE	2282 – 2013 BP
Roman	63 BC – 324 CE	2013 – 1626 BP
Byzantine	324 – 638 CE	1626 – 1312 BP
Early Islamic	638 – 1066 CE	1312 – 884 BP
Middle Islamic	1066-1492 CE	884 – 458 BP

Table 1. A chronological scheme for the Levant (after Finkelstein 2010 and 2011; Regev *et al.* 2012; Sharon 2013).

Code	Site Name	Latitude	Longitude	Elevation	Contributor	Site type	Chronological coverage	Reference
AKKO	Akko	32.91658	35.08695	3	Kaniewski	coastal	6000 – 0 BP	Kaniewski *et al.* 2013 and 2014
ALJOURD	Al Jourd	34.35	36.2	2100	Cheddadi	marsh	10800 – 0 BP	Cheddadi and Khater 2016
AMMIQ	Aammiq	33.76667	35.766	850	Cheddadi	wetland	11000 – 400 BP	Hajar *et al.* 2008
BIRKAT	Birkat Ram	33.23253	35.7663	940	Miebach	lake	6400 – 0 BP	Neumann *et al.* 2007
CHAMSINE	Chamsine	33.73333	35.95	856	Cheddadi	wetland	11000 – 600 BP	Hajar *et al.* 2010
DS7	Dead Sea 7	31.49111	35.4297	-415	Leroy and EPD	off-shore site	2800 – 0 BP	Leroy 2010 and 2018
DOR	Dor	32.61743	34.9163	0	Langgut (Kadosh)	coast	11000 – 9400 BP	Kadosh *et al.* 2004
GEDI97	Ein Gedi	31.41889	35.3883	-415	Miebach	lake	10000 – 0 BP	Litt *et al.* 2012
HULA1 HULA 2	Huleh	33.10556	35.5283	70	Woldring	lake	11000 – 400 BP 11000 – 9200 BP	van Zeist *et al.* 2009
TYRE	Tyre	33.27806	35.2030	3	EPD	ancient harbour	2600 – 1600 BP	European Pollen Database
TELDAN	Tel Dan	33.25007	35.6536	209	Kaniewski	spring	4200 – 1800 BP	Kaniewski *et al.* 2017
SEAGALILEE	Sea of Galilee	32.8205	35.588	-211	Miebach	lake	9000 – 0 BP	Schiebel and Litt 2017
9509MARINE	9509_marine	32.03167	34.283	0	Langgut	marine	11000 – 0 BP	Langgut *et al.* 2011; Langgut 2018

Table 2. List of fossil pollen sites and their contributors.

	AP (%)	OJCV	API	Simpson diversity	Ruderal weeds + Grazing plants	Regional pastoral	^{14}C SPD	Count	Aoristic weight	Random	Soreq z-score	Jeita z-score
AP (%)	1											
OJCV	****0.51**	1										
API	****-0.60**	0.10	1									
Simpson	-0.02	***0.38**	-0.33	1								
Ruderal weeds + Grazing plants	***0.54**	0.29	****-0.42**	0.14	1							
Regional pastoral	****-0.76**	-0.11	****0.82**	-0.24	****-0.47**	1						
^{14}C SPD	****0.69**	****0.62**	****-0.46**	0.15	****0.61**	****-0.47**	1					
count	****0.64**	****0.74**	-0.11	-0.05	***0.39**	****-0.43**	****0.81**	1				
aoristic weight	****0.64**	****0.78**	-0.07	0.13	***0.45**	****-0.42**	****0.68**	****0.92**	1			
random	****0.64**	****0.75**	-0.08	0.14	***0.46**	****-0.43**	****0.68**	****0.90**	****0.97**	1		
Soreq z-score	****-0.42**	****-0.55**	0.10	0.07	-0.31	0.33	***-0.35**	****-0.57**	****-0.68**	****-0.66**	1	
Jeita z-score	****-0.61**	****-0.69**	0.31	0.07	****-0.51**	****0.53**	****-0.71**	****-0.81**	****-0.81**	****-0.79**	****0.65**	1

Table 3. Spearman's Rank Correlation Coefficient (R-values) value matrix for the period 11000-600 cal. yr. BP (to 2600 cal. yr. BP for ^{14}C SPD). Significant correlations are indicated by bold numbers (**p*-value <0.05, ***p*-value <0.01).

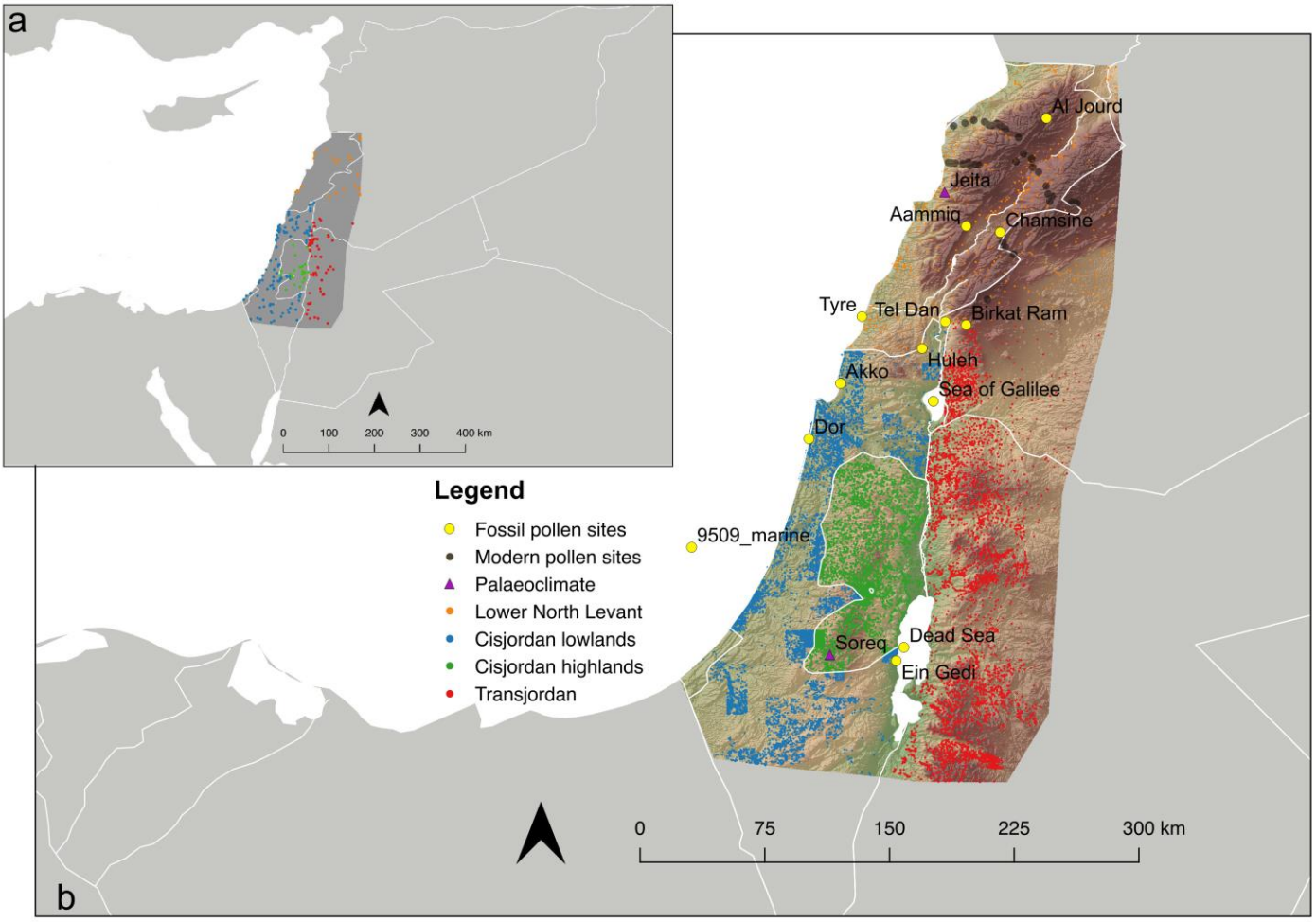

Figure 1. Map showing the distribution of a) sites with radiocarbon dates; b) archaeological sites, pollen records and palaeoclimate proxies.

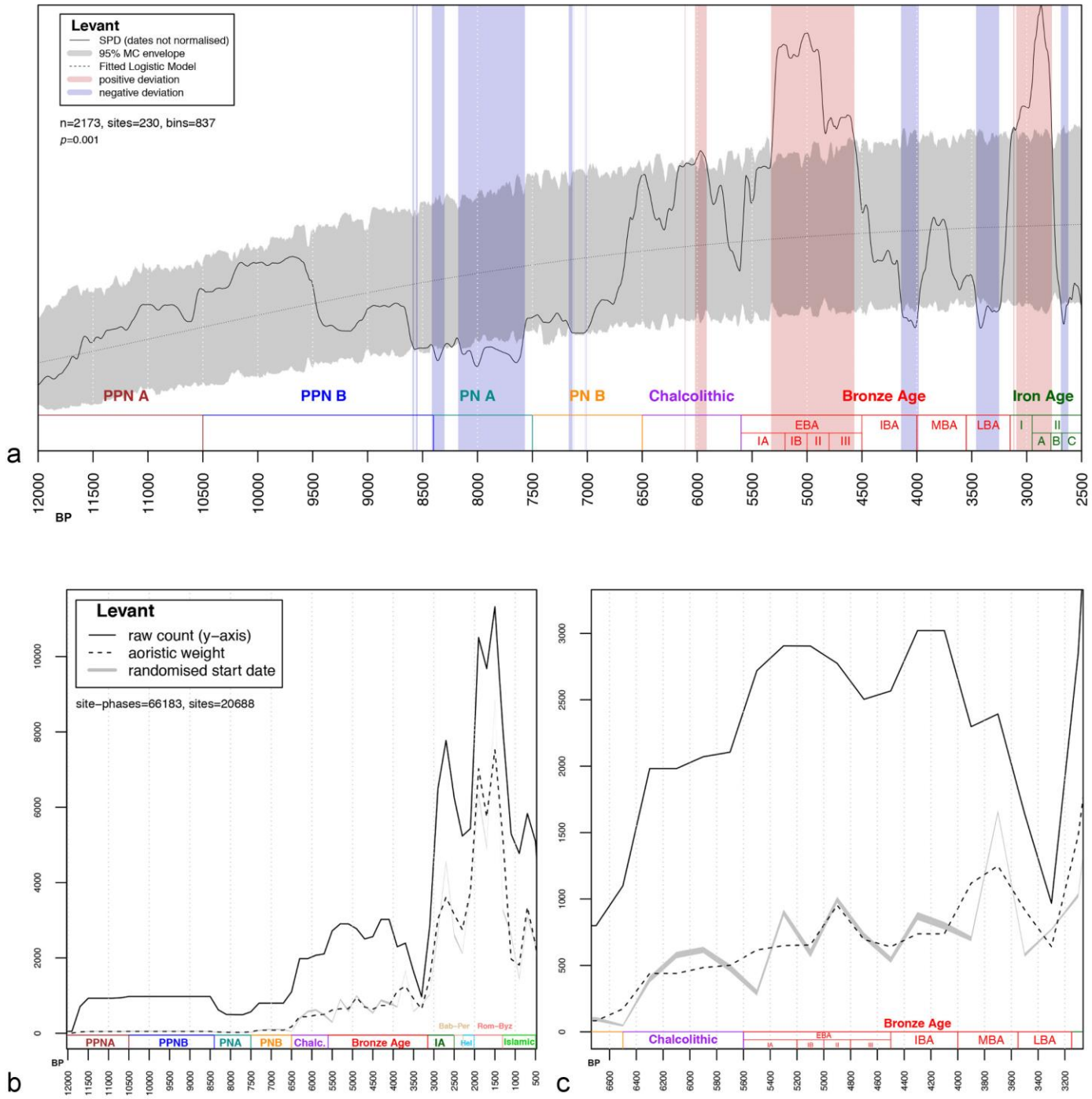

Fig. 2. a) Summed Probability Distribution (SPD) of unnormalised calibrated radiocarbon dates vs. a fitted logistic null model (95 % confidence grey envelope). Blue and red vertical bands indicate respectively chronological ranges within the observed SPD deviates negatively and positively from the null model. **b)** Comparison of sites raw count (solid line), aoristic sum (dashed line), and randomised start date of sites (grey envelope) from 12000 to 600 cal. yr. BP. **c)** Inset of population change between 6600 and 3000 cal. yr. BP.

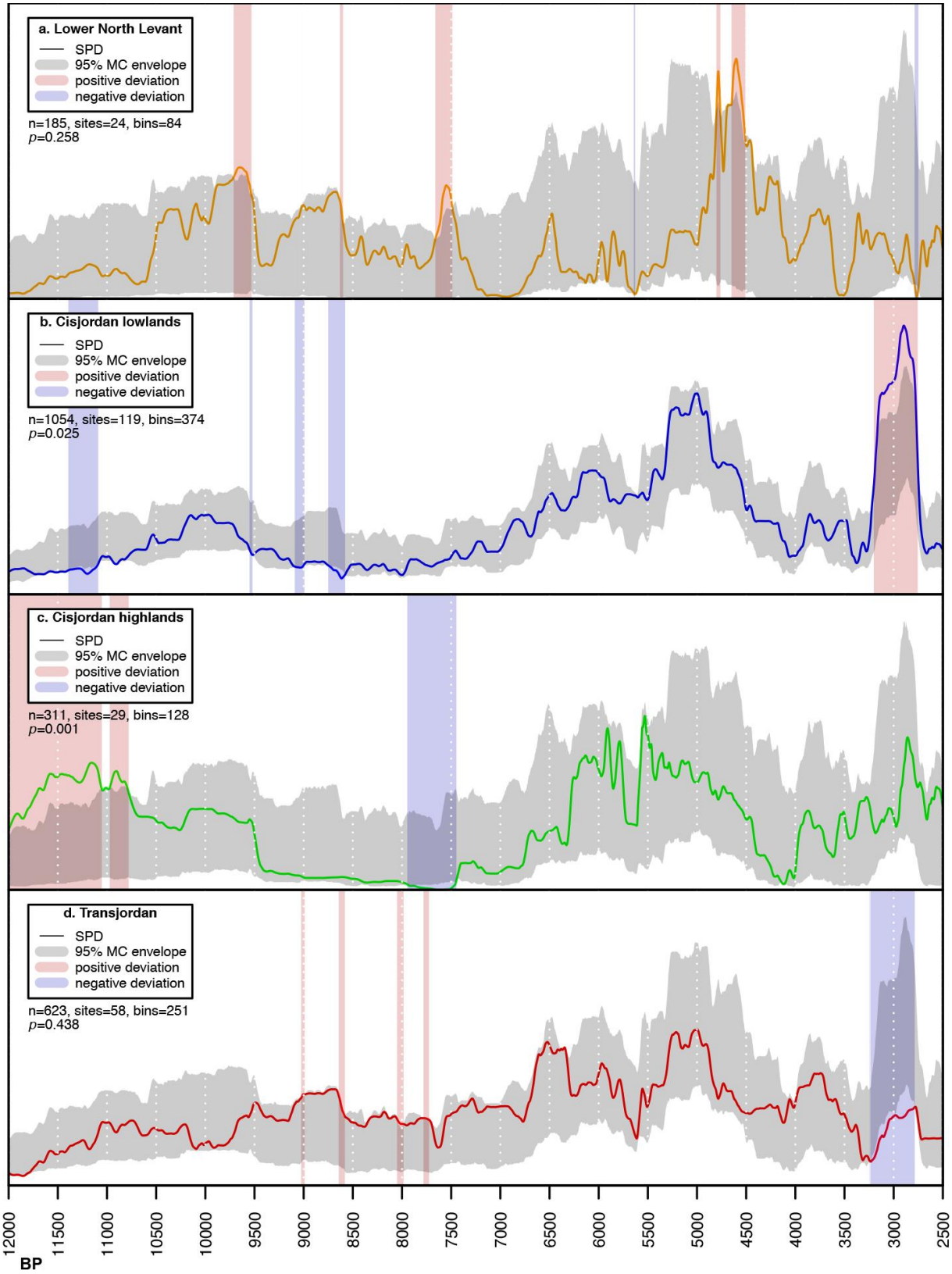

Figure 3. Regional summed probability distributions (SPDs) of calibrated radiocarbon dates for **(a)** Lower North Levant, **(b)** Cisjordan lowlands, **(c)** Cisjordan highlands, and **(d)** Transjordan compared with a 95% Monte Carlo envelope of the pan-regional model produced via permutation of sub-regional dates.

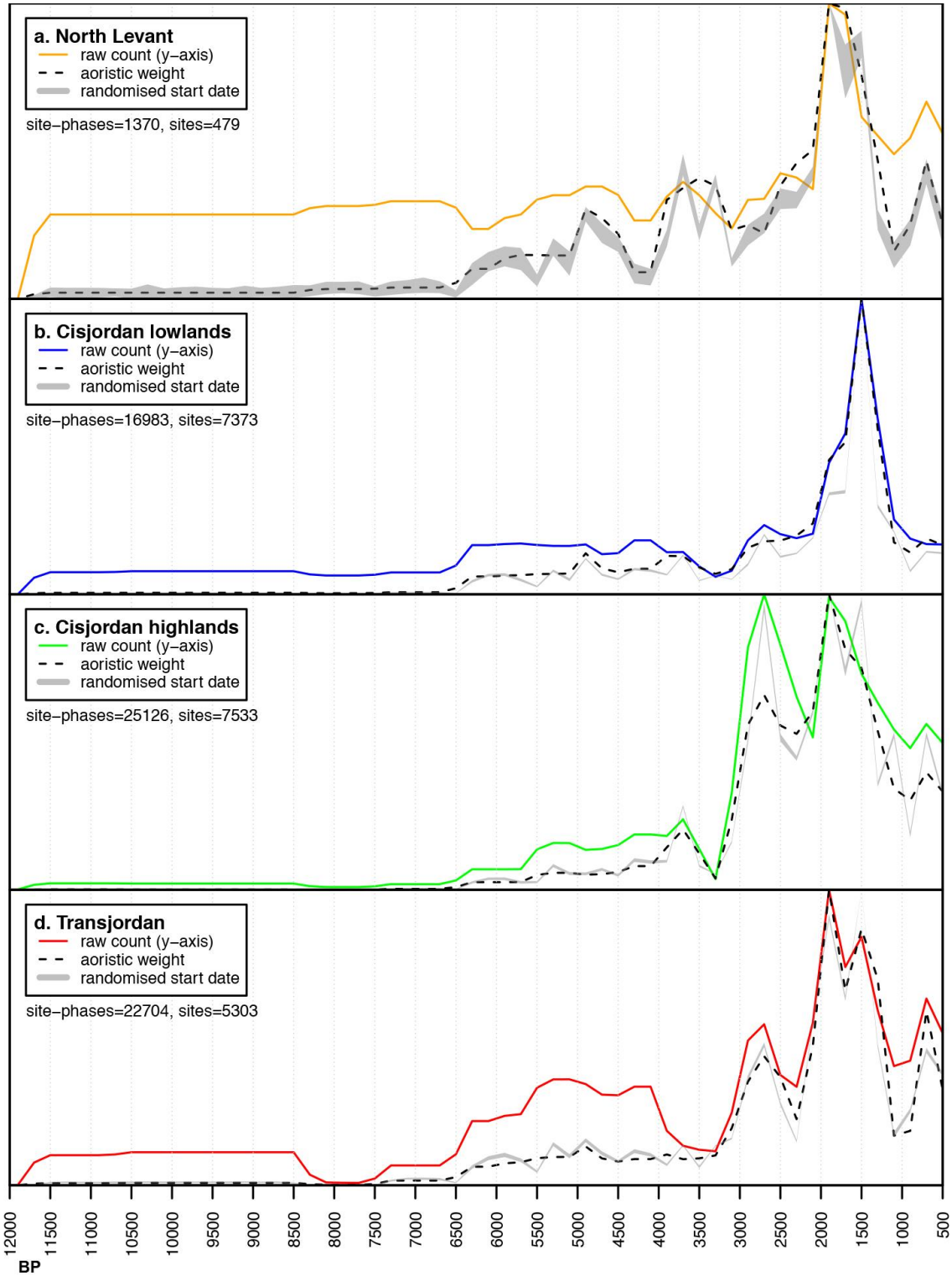

Figure 4. Regional comparison of sites raw count (solid line), aoristic sum (dashed line), and randomised start date of archaeological sites (grey envelope) for **(a)** Lower North Levant, **(b)** Cisjordan lowlands, **(c)** Cisjordan highlands, and **(d)** Transjordan.

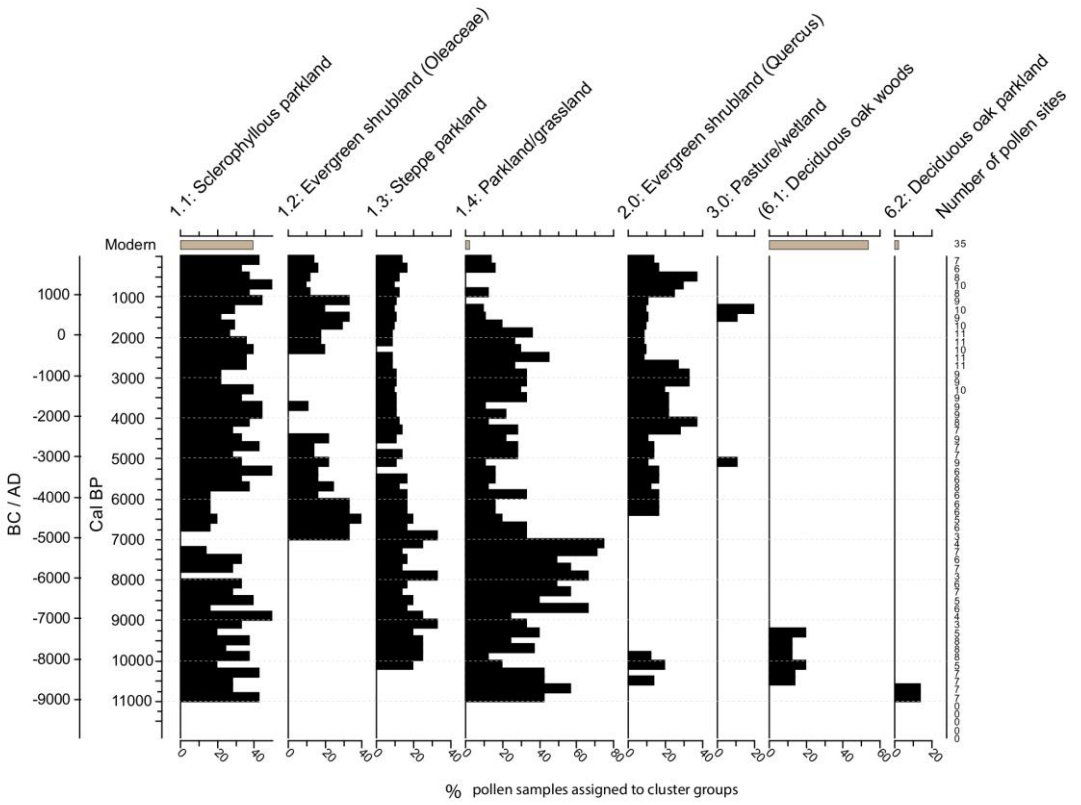

Figure 5. Pollen-inferred vegetation cluster groups (11,000 BP – modern) for the Levant.

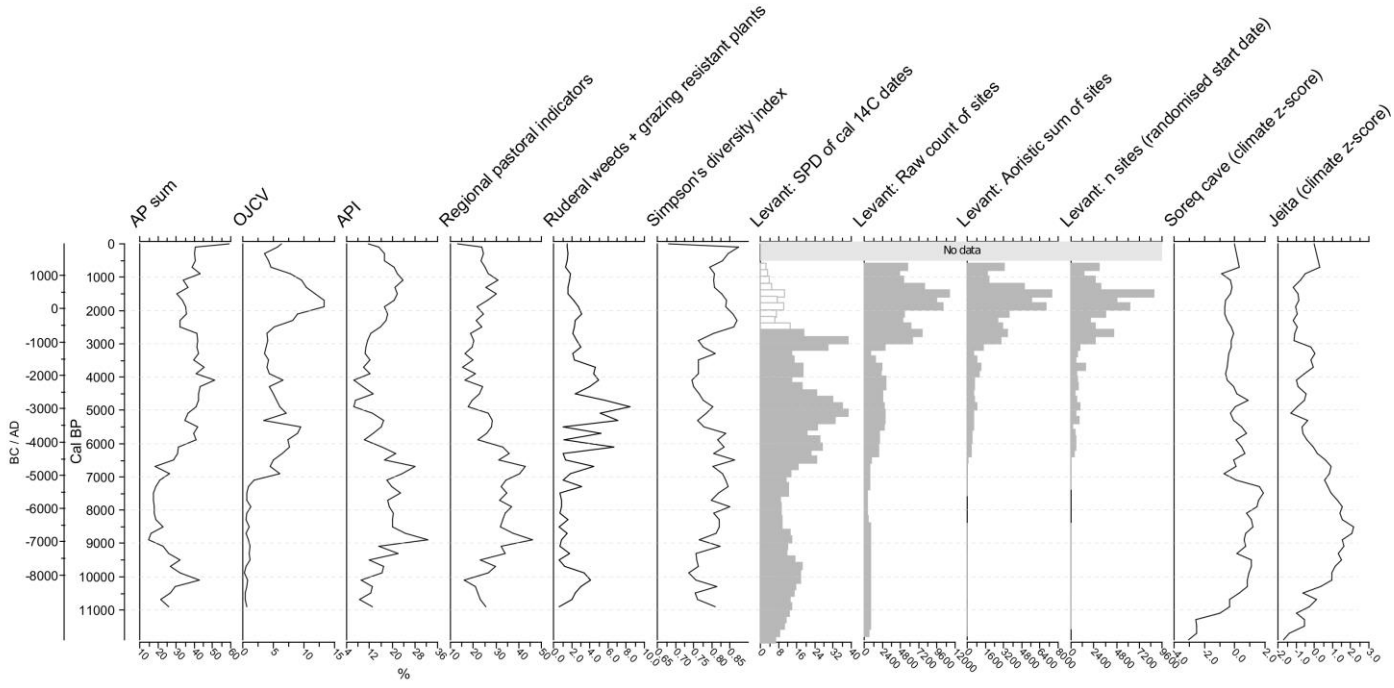

Figure 6. Pollen inferred indicator groups: arboreal pollen (%AP), sum of Olea, *Juglans*, *Castanea* and *Vitis* (OJCV), anthropogenic pollen index (API), Ruderal weeds + grazing resistant plants, pastoral indicators and Simpson's diversity Index averaged for all sites in the study area (11,000 BP to modern) compared with proxy archaeological data and palaeoclimate records from Soreq and Jeita's caves. Time windows with insufficient radiocarbon dates for reliable SDP of calibrated ^{14}C dates are shown in white.

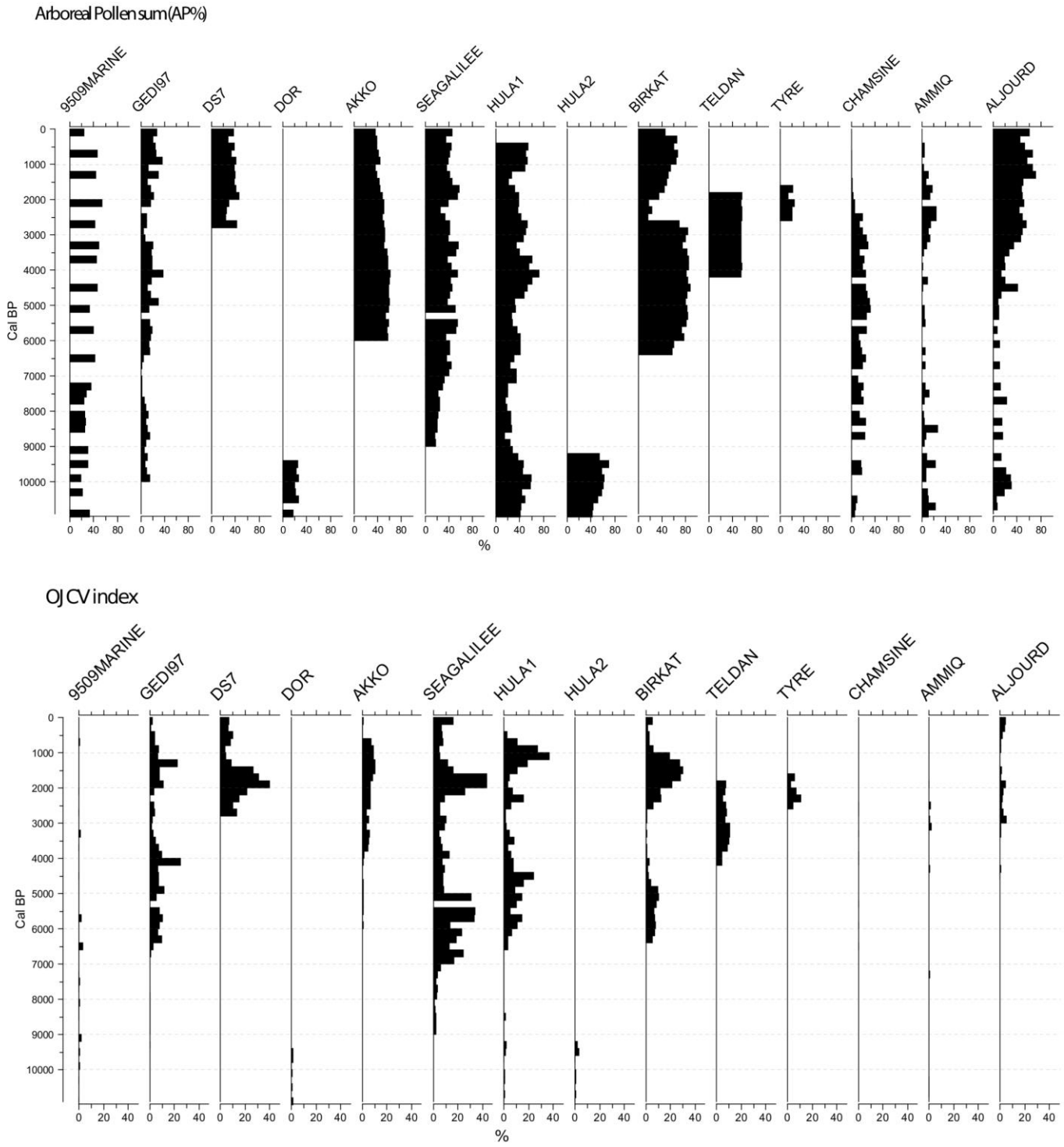

Figure 7. Pollen inferred indicator groups at a site-level scale: arboreal pollen (AP%), and sum of *Olea*, *Juglans*, *Castanea* and *Vitis* (OJCV). Sites ordered from left to right according to a South-North gradient.

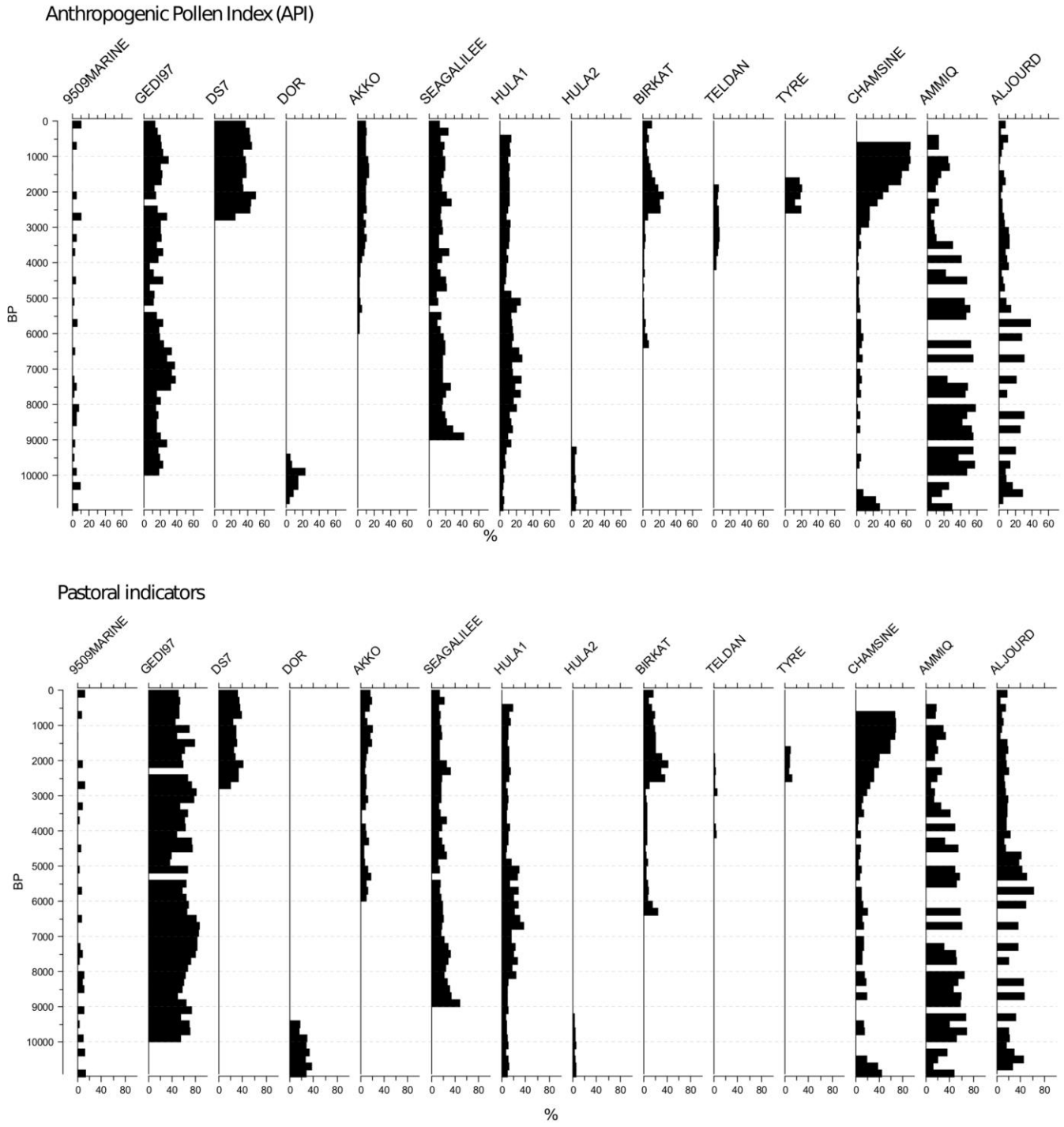

Figure 8. Pollen inferred indicator groups at a site-level scale: anthropogenic pollen index (API), and regional pastoral indicators. Sites ordered from left to right according to a South-North gradient.

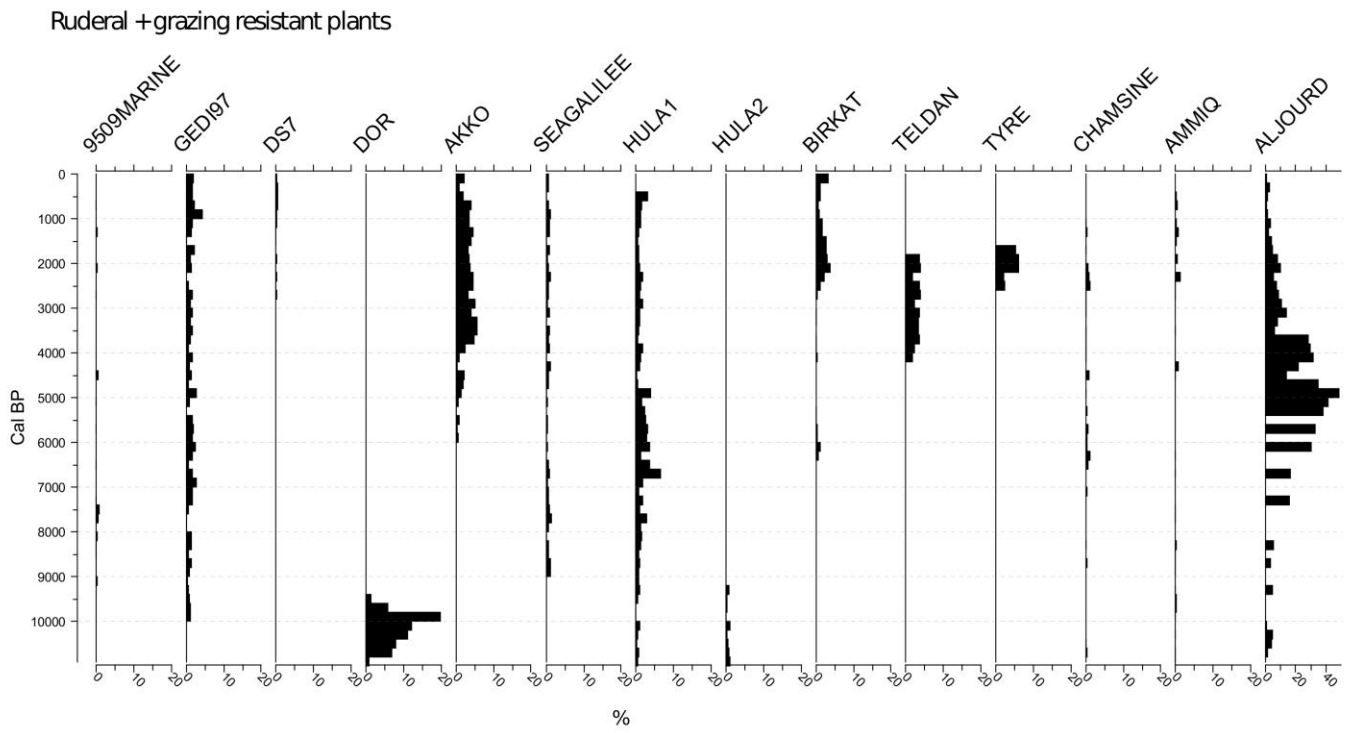

Figure 9. Pollen inferred indicator groups at a site-level scale: ruderal weeds + grazing resistant plants. Sites ordered from left to right according to a South-North gradient.

Supplemental material 1

Radiocarbon dates from archaeological sites were compiled from existing online databases and electronic and print. A total of 2,173 uncalibrated radiocarbon dates from 230 sites have been collected. Below the sources from which the radiocarbon dates have been collected.

Databases/Datasets

BANADORA. Banque Nationale de Données Radiocarbonne pour l'Europe et le Proche Orient, Centre de Datation par le Radiocarbonne, CNRS Lyon: http://www.arar.mom.fr/banadora/

CalPal - The Cologne Radiocarbon Calibration & Palaeoclimate Research Package. Developed by Weninger, B., Jöris, O., and Danzeglocke, U: http://monrepos-rgzm.de/forschung/ausstattung.html#calpal

EX ORIENTE - PPND - the Platform for Neolithic *Radiocarbon* Dates: https://www.exoriente.org/associated_projects/ppnd.php

EUROEVOL. Manning, K; Timpson, A; Colledge, S; Crema, E; Shennan, S; (2015) The Cultural Evolution of Neolithic Europe. EUROEVOL Dataset: http://discovery.ucl.ac.uk/1469811/

IRPA/KIK. Royal Institute for Cultural Heritage web based Radiocarbon database. Van Strydonck, M. and De Roock, E., 2011. Royal Institute for Cultural Heritage web-based radiocarbon database. *Radiocarbon*, *53*(2), pp.367-370. http://c14.kikirpa.be/

ORAU. Oxford Radiocarbon Accelerator Unit online database: https://c14.arch.ox.ac.uk/databases.html

RADON. Martin Hinz, Martin Furholt, Johannes Müller, Dirk Raetzel-Fabian, Christoph Rinne, Karl-Göran Sjögren, Hans-Peter Wotzka, RADON - Radiocarbon dates online 2012. Central European database of ^{14}C dates for the Neolithic and Early Bronze Age. www.jungsteinsite.de, 2012, 1-4: http://radon.ufg.uni-kiel.de/

References

Al-Bashaireh, K. and Al-Muheisen, Z., 2011. Subsistence strategies and palaeodiet of Tell al-Husn, northern Jordan: nitrogen and carbon stable isotope evidence and radiocarbon dates. *Journal of Archaeological Science 38*(10), 2606-2612.

Ambers, J. and Bowman, S., 2003. Radiocarbon measurements from the British Museum: datelist XXVI. *Archaeometry 45*(3), 531-540.

Anderson, R.W., 2006. Southern Palestinian chronology: two radiocarbon dates for the Early Bronze Age at Tell el-Hesi (Israel). *Radiocarbon 48*(1), 101-107.

Anfinset, N., Taha, H., al-Zawahra, M. and Yasine, J., 2011. Societies in transition: contextualizing Tell el-Mafjar, Jericho. *Culture, Chronology and the Chalcolithic. Levant Supplementary Series 9*, 97-113.

Arranz-Otaegui, A., Colledge, S., Ibañez, J.J. and Zapata, L., 2016. Crop husbandry activities and wild plant gathering, use and consumption at the EPPNB Tell Qarassa North (south Syria). *Vegetation history and archaeobotany 25*(6), 629-645.

Asscher, Y., Lehmann, G., Rosen, S.A., Weiner, S. and Boaretto, E., 2015. Absolute dating of the Late Bronze to Iron Age transition and the appearance of Philistine culture in Qubur el-Walaydah, southern Levant. *Radiocarbon 57*(1), 77-97.

Avner, U. and Carmi, I., 2001. Settlement Patterns in the Southern Levant Deserts During the 6th–3rd Millennia BC: a Revision Based on 14 C Dating. *Radiocarbon 43*(3), 1203-1216.

Badreshany, K. and Kamlah, J., 2013. Middle Bronze Age pottery from Tell el-Burak, Lebanon. *Berytus 53*, 81-113.

Balbo, A.L., Iriarte, E., Arranz, A., Zapata, L., Lancelotti, C., Madella, M., Teira, L., Jiménez, M., Braemer, F. and Ibáñez, J.J., 2012. Squaring the circle. Social and environmental implications of pre-pottery neolithic building technology at Tell Qarassa (South Syria). *PloS one 7*(7), p.e42109.

Banning, E.B., Siggers, J. and Rahimi, D., 1994. The Late Neolithic of the southern Levant: hiatus, settlement shift or observer bias? The perspective from Wadi Ziqlab. *Paléorient 33.1*, 151-164.

Bar-Yosef, O., 1988. Le Paléolithique d'Israël. L' *Anthropologie 92*(3), 769-795.

Bar-Yosef, O. and Valla, F.R., 1979. L'evolution du Natoufien nouvelles suggestions. *Paléorient 5*, 145-152.

Bar-Yosef, O. and Vogel, J.C., 1987. Relative and absolute chronology of the Epipalaeolithic in the southern Levant. *Chronologies in the Near East*, 219-46.

Belfer-Cohen, A. and Goring-Morris, A.N., 2005. Which way to look? conceptual frameworks for understanding Neolithic processes. *Dialogue on the Early Neolithic origin of ritual centers. Neo-Lithics 2*(05), pp.22-24.

Blackham, M., 1997. Changing Settlement at Tabaqat al-Bûma in Wadi Ziqlab, Jordan: A Stratigraphic Analysis. In: Gebel H.G.K. , Kafafi Z. and Rollefson G.O. (Eds.*), The Prehistory of Jordan II. Perspectives from 1997*. Berlin: ex oriente (Studies in Early Near Eastern Production, Subsistence and Environment 4), 345-360.

Boaretto, E., Bar-Yosef, O, Gopher, A., Goring-Morris, A. N., and Kozlowski, S. K., 2010a. *Gilgal: Early Neolithic occupations in the lower Jordan Valley: the excavations of Tamar Noy*. Oakville CT: Oxbow Books Limited, 33-38.

Boaretto, E., Finkelstein, I. and Shahack-Gross, R., 2010b. Radiocarbon results from the Iron IIA site of Atar Haroa in the Negev Highlands and their archaeological and historical implications. *Radiocarbon 52*(1), 1-12.

Bonani G, Wölfli W., 1991. Radiocarbon dates from area B. In: Kempinski, A. and Niemeier, W.D. (Eds.), *Excavations at Kabri: Preliminary Report of 1990 Season 5*. Tell Aviv: Tell Kabri Expedition Tel Aviv University, 8.

Borrell, F., Boaretto, E., Caracuta, V., Cohen-Sasson, E., Lavi, R., Lpui, R., Teira, L., and Vardi, J., 2015. Nahal Efe A Middle Pre-Pottery Neolithic B Site in the North-eastern Negev Preliminary Results of the 2015 Pilot Season. *Neo-Lithics 2/15*, 33-41.

Bourke, S.J. and Zoppi, U., 2007. *Dating the Cultic Assemblages from the Bronze Age Fortress Temple Complex at Pella in Jordan*. Progress Report for AINGRA 05013. Sydney: University of Sydney.

Bourke, S., Zoppi, U., Meadows, J., Hua, Q. and Gibbins, S., 2009. The beginning of the Early Bronze Age in the north Jordan Valley: new 14 C determinations from Pella in Jordan. *Radiocarbon 51*(3), 905-913.

Braidwood, R. J., 1958. Near Eastern Prehistory. The swing from food-collecting cultures to village-farming communities is still imperfectly understood. *Science 127,* 1419-1430.

Braun, E., 2001. Proto, Early Dynastic Egypt, and Early Bronze I-II of the Southern Levant: Some Uneasy 14 C Correlations. *Radiocarbon 43*(3), 1279-1295.

Braun, E., Van Den Brink, E.C., Regev, J., Boaretto, E. and Bar, S., 2013. Aspects of Radiocarbon Determinations and the Dating of the Transition from the Chalcolithic Period to Early Bronze Age I in the Southern Levant. *Paléorient 39*(1), 23-46.

Bronk Ramsey, C., Higham, T. F. G., Brock, F., Baker, D., & Ditchfield, P., 2009. Radiocarbon dates from the oxford ams system: archaeometry datelist 33. A*rchaeometry 51*(2), 323-349.

Bronk Ramsey, C., Higham, T., Brock, F., Baker, D., Ditchfield, P., & Staff, R., 2015. Radiocarbon Dates from the Oxford AMS System: Archaeometry Datelist 35. A*rchaeometry, 57*(1), 177-216.

Bruins, H.J., Mazar, A. and van der Pflicht, J., 2007. *The end of the 2nd millennium BCE and the transition from Iron I to Iron IIA: radiocarbon dates of Tel Rehov, Israel* (Vol. 37, pp. 79-100). Verlag der Österreichischen Akademie der Wissenschaften.

Burleigh, R., 1981. Appendix C: Radiocarbon dates. In: Kenyon, K. M. (Ed.), *Excavations at Jericho.* Volume 3. *The Architecture and Stratigraphy of the Tell.* London: The British School of Archaeology in Jerusalem, 501-504.

Burleigh, R., 1983. Appendix D: Radiocarbon dates. In: Kenyon, K. M. AND Holland T. A. (Eds.), *Excavations at Jericho.* Volume 5. *The Pottery Phases of the Tell and Other Finds*. London: The British School of Archaeology in Jerusalem, 760-765.

Burton, M. and Levy, T.E., 2011. The end of the Chalcolithic period (4500–3600) in the northern Negev Desert, Israel. In: J. L. Lovell and Y. M. Rowan (Eds.), *Culture, Chronology and the Chalcolithic. Theory and Transition.* Oxford: Oxbow, 178-191.

Byrd, B.F., 1989. The Natufian: settlement variability and economic adaptations in the Levant at the end of the Pleistocene. *Journal of World Prehistory 3*(2), pp.159-197.

Carmi, I. and Segal, D., 1992. Rehovot Radiocarbon Measurements IV 1. *Radiocarbon 34*(1), pp.115-132.

Churcher, C.S., 1994. The vertebrate fauna from the Natufian level at Jebel es-Saaïdé (Saaïdé II), Lebanon. *Paléorient*, 35-58.

Clare, L., 2010. Pastoral clashes: Conflict risk and mitigation at the Pottery Neolithic transition in the Southern Levant. *Neo-Lithics, 1*(10), pp.13-31.

Conrad, N., 2002. An overview of the recent excavations at Baaz Rockshekter, Damascus Province, Syria. In: Korfmann, M. and Aslan, R. (Eds.), *Mauerschau: Festschrift für Manfred Korfmann*. Remshalden-Grunback: Greiner, vol.2, 623-640.

Contenson, H., De, 1975. Les fouilles à Ghoraifé en 1974. *Annales Archéologiques de Syrie,* 25, 17-32.

Dee, M., Higham, T.F.G. and Postgate, N., 2017. Section 2: The 14C determinations. In Excavations at Kilise Tepe 2007-2011: The Late Bronze and Iron Ages. University of Cambridge. doi:10.17863/CAM.10130

Dever, W. G, Lance, H. D, Ballard, R. G, and Cole, D. P., 1974. Gezer II: Report of the 1967 70 Seasons in Fields I and II. Jerusalem: Hebrew Union Coll/Nelson Glueck School Biblical Archaeology.

Edwards, P. C., 2001. Nine millennia by Lake Lisan: the Epipalaeolithic in the East Jordan Valley between 20,000 and 11,000 years ago. In: *Studies in the History and Archaology oj Jordan VII.* Amman: Department of Antiquities of Jordan, 85-93.

Edwards, P.C., Bocquentin, F., Colledge, S.M., Edwards, Y., Le Dosseur, G., Martin, L., Stanin, Z. and Webb, J., 2013. Wadi Hammeh 27: an Open-air 'Base-camp'on the Fringe of the Natufian 'Homeland'. In: F. Valla, O. Bar-Yosef (Eds.), *Natufian Foragers in the LevantPublisher: International Monographs in Prehistory*. Ann Arbor: International Monographs in Prehistory, 319-348.

Falconer, S.E. and Fall, P.L., 2016. A radiocarbon sequence from Tell Abu en-Ni 'aj, Jordan and its implications for Early Bronze IV chronology in the Southern Levant. *Radiocarbon 58*(3), 615-647.

Falconer, S.E. and Fall, P.L., 2017. Radiocarbon Evidence from Tell Abu en-Ni'aj and Tell el-Hayyat, Jordan, and Its Implications for Bronze Age Levantine and Egyptian Chronologies. *Journal of Ancient Egyptian Interconnections13*, 7-19.

Fantalkin, A., Finkelstein, I. and Piasetzky, E., 2011. Iron Age Mediterranean chronology: a rejoinder. *Radiocarbon 53*(1), 179-198.

Finkelstein, I. and Piasetzky, E., 2007. Radiocarbon dating and Philistine chronology with an addendum on el-Ahwat. *Ägypten und Levante/Egypt and the Levant 17*, 73-82.

Finkelstein, I. and Piasetzky, E., 2010. The Iron I/IIA transition in the Levant: a reply to Mazar and Bronk Ramsey and a new perspective. *Radiocarbon 52*(4), 1667-1680.

Fischer, P., 2014. The Southern Levant (Transjordan) During the Late Bronze Age. In: Steiner, M.L. and Killebrew, A.E. (Eds.). *The Oxford Handbook of the Archaeology of the Levant: c. 8000-332 BCE*. Oxford: Oxford University Press.

Flohr, P., Fleitmann, D., Matthews, R., Matthews, W. and Black, S., 2016. Evidence of resilience to past climate change in Southwest Asia: Early farming communities and the 9.2 and 8.2 ka events. *Quaternary Science Reviews 136*, 23-39.

Garfinkel, Y. and Kang, H.G., 2011. The relative and absolute chronology of Khirbet Qeiyafa: very late Iron Age I or very early Iron Age IIA? *Israel Exploration Journal 61*, pp.171-183.

Garfinkel, Y., Streit, K., Ganor, S. and Reimer, P.J., 2015. King David's city at Khirbet Qeiyafa: results of the second radiocarbon dating project. *Radiocarbon 57*(5), pp.881-890.

Garrard, A. and Yazbeck, C., 2013. The Natufian of Moghr el-Ahwal in the Qadisha Valley, Northern Lebanon. In: Bar-Yosef, O. and F, Valla (Eds.), *Natufian Foragers in the Levant. Terminal Pleistocene Social Changes in Western Asia*. Ann Arbor: International Monographs in Prehistory, 17-27.

Genz, H., 2002. Die frühbronzezeitliche Keramik von Hirbet ez-Zeraqon: mit Studien zur Chronologie und funktionalen Deutung frühbronzezeitlicher Keramik in der südlichen Levante. Wiesbaden: Harrasowitz Verlag.

Gibbs, K., Kadowaki, S. and Banning, E.B., 2010. Excavations at al-Basatin, a late Neolithic and Early Bronze I site in Wadi Ziqlab, northern Jordan. *Annual of the Department of Antiquities of Jordan 54*, pp.461-476.

Gilead, I., 1988. The Chalcolithic period in the Levant. *Journal of World Prehistory 2*(4), pp.397-443.

Gilead, I., 1991. The upper Paleolithic period in the Levant. *Journal of World Prehistory 5*(2), pp.105-154.

Gopher, A. and Gophna, R., 1993. Cultures of the Eighth and Seventh Millennia BP in the Southern Levant: A Review for the 1990s. *Journal of World Prehistory 7*(3), 297-353.

Gopher, A., Lemorini, C., Boaretto, E., Carmi, I., Barkai, R. and Schechter, H.C., 2013. Qumran Cave 24, a Neolithic-Chalcolithic site by the Dead Sea: A short report and some information on lithics. In: Borrell, F., Ibáñez, J.J. and Molist, M., 2014. *Stone Tools in Transition: From Hunter-Gatherers to Farming Societies in the Near East*. Barcelona: Servei de Publicacions de la Universitat Autònoma de Barcelona, pp.101-114.

Goring-Morris, A.N., 1987. *At the edge: terminal Pleistocene hunter-gatherers in the Negev and Sinai*. Oxford: BAR International Series 361.

Goring-Morris, A. N., 1991. The Harifian of the Southern Levant. In: O. Bar-Yosef and F. R. Valla (Eds.), *The Natufian Culture in the Levant*. Ann Arbor: International Monographs in Prehistory, pp. 173–216.

Gowlett, J.A., 1987. The archaeology of radiocarbon accelerator dating. *Journal of World Prehistory*, *1*(2), pp.127-170.

Gregoricka, L.A. and Sheridan, S.G., 2017. Continuity or conquest? A multi-isotope approach to investigating identity in the Early Iron Age of the Southern Levant. *American journal of physical anthropology 162*(1), pp.73-89.

Grosman, L., Munro, N.D., Abadi, I., Boaretto, E., Shaham, D., Belfer-Cohen, A. and Bar-Yosef, O., 2016. Nahal Ein gev II, a late natufian community at the sea of galilee. *PloS one 11*(1), p.e0146647.

Hadas, G., Liphschitz, N. and Bonani, G., 2005. Two ancient wooden anchors from Ein Gedi, on the Dead Sea, Israel. *International Journal of Nautical Archaeology 34*(2), pp.299-307.

Harrison, T.P. and Barlow, C., 2005. Mesha, the Mishor, and the Chronology of Iron Age Madaba. In: Levy, T. and Higham, T., 2005. *The Bible and radiocarbon dating: archaeology, text and science*. London: Routledge, 179-190.

Höflmayer, F., Dee, M.W., Genz, H. and Riehl, S., 2014. Radiocarbon evidence for the Early Bronze Age Levant: the site of Tell Fadous-Kfarabida (Lebanon) and the end of the Early Bronze III period. *Radiocarbon 56*(2), pp.529-542.

Höflmayer, F., Kamlah, J., Sader, H., Dee, M.W., Kutschera, W., Wild, E.M. and Riehl, S., 2016. New evidence for Middle Bronze Age chronology and synchronisms in the Levant: Radiocarbon dates from Tell el-Burak, Tell el-Dabʿa, and Tel Ifshar compared. *Bulletin of the American Schools of Oriental Research* 375, pp.53-76.

Holdorf, P.S., 2010. Comparison of EB IV radiocarbon results from Khirbat Iskandar and Bab adh-Dhra. In: S. Richard et al. 2010 (Eds.), *Archaeological Expedition to Khirbat Iskander and its Environs, Jordan: Khirbat Iskander: Final Report on the Early Bronze IV Area C 'Gateway' and Cemeteries.* Boston: American Schools of Oriental Research, 267-270.

Housley, R.A., 1994. Eastern Mediterranean chronologies. The Oxford AMS contribution. *Radiocarbon 36*, pp.55-73.

Jull, A. J. T., Donahue, D. J., Carmi, I, and Segal, D., 1998. In: Schick, T., 1998. *The Cave of the Warrior: a fourth millennium burial in the Judean Desert* (No. 5). Jerusalem: Israel Antiquities Authorit, 110-113.

Kadowaki, S., Gibbs, K., Allentuck, A. and Banning, E.B., 2008. Late Neolithic Settlement in Wadi Ziqlab, Jordan: al-Basatîn. *Paléorient 34* (1), pp.105-129.

Kafafi, Z., 1993. The Yarmoukians in Jordan. *Paléorient 19*, pp.101-114.

Korfmann, M. and Aslan, R., 2002. *Mauerschau: Festschrift für Manfred Korfmann*. Greiner.

Kuijt, I., 1994. Pre-Pottery Neolithic A settlement variability: evidence for sociopolitical developments in the southern Levant. *Journal of Mediterranean Archaeology 7*(2), pp.165-192.

Kuijt, I., 2001. Lithic inter-assemblage variability and cultural-historical sequences: A consideration of the Pre-Pottery Neolithic A occupation of Dhra', Jordan. *Paléorient 27*(1), pp.107-125.

Kuijt I., Bar-Yosef O., 1994. Radiocarbon chironology for the Levantine Neolithic: Observations and data. In: Bar-Yosef O., Kra R. (Eds.), *Late Quatemary Chronology and Paleoclimates of the Eastern Mediterranean*. Cambridge. MA: Radiocarbon and the Peabody Museum, 227-246.

Kuijt, I. and Goodale, N.B., 2006. Chronological frameworks and disparate technology: An exploration of chipped stone variability and the forager to farmer transition at'Iraq Ed-Dubb, Jordan. *Paléorient 32*(1), pp.27-45.

Lawn, B., 1974. University of Pennsylvania radiocarbon dates XVII. *Radiocarbon 16*(2), pp. 219-237.

Lombardo, M., and Piloto, A., 2000. New Radiocarbond dates and assessment of all dates obtained for the Early and Middle Bronze Ages in Jericho. In: Marchetti, N. and Nigro, L. (eds.), *Excavations at Jericho, 1998, Preliminary Report on the Second Season of Archaeological Excavations and Surveys at Tell es-Sultan, Palestine*. Roma: Universita' di Roma La Sapienza, 329-332.

Lorentzen, B., Manning, S.W. and Kahanov, Y., 2014. The 1st millennium AD Mediterranean shipbuilding transition at Dor/Tantura Lagoon, Israel: dating the Dor 2001/1 shipwreck. *Radiocarbon 56*(2), 667-678.

Lovell, J.L., Meadows, J. and Jacobsen, G.E., 2010. Upland olive domestication in the Chalcolithic period: new 14 C determinations from el-Khawarij (Ajlun), Jordan. *Radiocarbon 52*(2), 364-371.

Maher, L.A., Banning, E.B. and Chazan, M., 2011. Oasis or mirage? Assessing the role of abrupt climate change in the prehistory of the southern Levant. *Cambridge Archaeological Journal 21*(1), 1-30.

Marcus, E. S., 2013. Correlating and combining Egyptian historical and southern Levantine radiocarbon chronologies at Middle Bronze Age IIa Tel Ifshar, Israel. In: Shortland A. J. and Bronk Ramsey C. (Eds.), *Radiocarbon and the Chronologies of Ancient Egypt*. Oxford: Oxbow Books, 182-208.

Mazar, A. and Rotem, Y., 2009. Tel Beth Shean during the EB IB period: evidence for social complexity in the late 4th millennium BC. *Levant 41*(2), pp.131-153.

Mazar, A., de Miroschedji, P. and Porat, N., 1996. Hartuv, an aspect of the Early Bronze I culture of southern Israel. *Bulletin of the American Schools of Oriental Research 302*, pp.1-40.

Mazar, A., Bruins, H.J., Panitz-Cohen, N. and Van der Plicht, J., 2005. Ladder of time at Tel Rehov: stratigraphy, archaeological context, pottery and radiocarbon dates In: Levy, T. and Higham, T., 2005. *The Bible and radiocarbon dating: archaeology, text and science*. London: Routledge, pp.193-255.

Murphy, T.M., Ben-Yehuda, N., Taylor, R.E. and Southon, J.R., 2011. Hemp in ancient rope and fabric from the Christmas Cave in Israel: talmudic background and DNA sequence identification. *Journal of archaeological science 38*(10), 2579-2588.

Nawrocka, D.M., Michczyńska, D.J., Pazdur, A. and Czernik, J., 2007. Radiocarbon chronology of the ancient settlement in the Golan Heights area, Israel. *Radiocarbon 49*(2), 625-637.

Oren E., Yekutieli Y., 1992. Taur Ikhbeineh; earliest evidence for Egyptian interconnection. In: van den Brink E. C. M. (Ed.), The Nile Delta in Transition: 4th - 3rd Millennium BC. Jerusalem: Israel Exploration Society, 361-84

Paz, S., 2010. Life in the City: *The Birth of an Urban Habitus in the Early Bronze Age of Israel*. Unpublished PhD Thesis, Tel Aviv University (in Hebrew).

Pinhasi, R., Fort, J. and Ammerman, A.J., 2005. Tracing the origin and spread of agriculture in Europe. *PLoS biology 3*(12), p.e410.

Rasmussen, K.L., Gunneweg, J., van der Plicht, J., Kralj Cigić, I., Bond, A.D., Svensmark, B., Balla, M., Strlic, M. and Doudna, G., 2011. On the age and content of jar-35 – a sealed and intact storage jar found on the southern plateau of Qumran. *Archaeometry 53*(4), 791-808.

Rech, J.A., Fischer, A.A., Edwards, D.R. and Jull, A.T., 2003. Direct dating of plaster and mortar using AMS radiocarbon: a pilot project from Khirbet Qana, Israel. *Antiquity 77*(295), pp.155-164.

Regev, L., Eckmeier, E., Mintz, E., Weiner, S. and Boaretto, E., 2011. Radiocarbon concentrations of wood ash calcite: potential for dating. *Radiocarbon 53*(1), 117-127.

Regev, J., De Miroschedji, P. and Boaretto, E., 2012a. Early Bronze Age chronology: radiocarbon dates and chronological models from Tel Yarmuth (Israel). *Radiocarbon 54*(3-4), pp. 505-524.

Regev, J., Finkelstein, I., Adams, M. J., and Boaretto, E., 2014. Wiggle Matched C14 Chronology of Early Bronze Megiddo and the Synchronization of Egyptian and Levantine Chronologies. *Egypt and the Levant 24*, 243-266.

Regev, J., Regev, L., Mintz, E. and Boaretto, E., 2017. Radiocarbon Assessment of Early Bronze Arad: The 20 Year Lifespan of Stratum II. *Tel Aviv 44*(2), pp.165-177.

Rollefson, Gary O., Simmons, Alan H., and Kafafi, Zeidan (1992), 'Neolithic cultures at 'Ain Ghazal'. *Journal of Field Archaeology 19* (4), 443-70.

Rollefson, G. O., 1998. The Aceramic Neolithic. In: D. O. Henry (Ed.) 1998, The Prehistoric Archaeology of Jordan. Oxford: BAR International Series 705, pp.102-126.

Saidah, R., 1979. Fouilles de Sidon-Dakerman: L´ agglomération chalcolithique. *Berytus: Archaeological Studies* 27, pp. 29-56.

Sayej, G., 2007. Lithic variability among the PPNA assemblages of the Dead Sea Basin. In: L. Astruc, D. Binder and F. Briois (Eds.), Systèmes techniques et communautés du Néolithique précéramique au Proche-Orient (Technical Systems and Near Eastern PPNA Communities), pp 87-102. APDCA: Antibes – France.

Schick, T., 1998. *The Cave of the Warrior: a fourth millennium burial in the Judean Desert* (No. 5). Israel Antiquities Authority.

Segal, D., & Carmi, I. (1996). Rehovot Radiocarbon Date List V. *'Atiqot, 29*, 79-106.

Segal, D. and Carmi, I., 2003. Radiocarbon dates from Horbat Hani (West). *ʻAtiqot 44*, 65-66.

Segal, D., and Carmi, I., 2006. Radiocarbon dates. In: Getzov (Ed.), *The Tel Bet Yerah Excavations, 1994-1995*. Jerusalem: Israel Antiquities Authority, 175-176.

Shai, I., Greenfield, H.J., Regev, J., Boaretto, E., Eliyahu-Behar, A. and Maeir, A.M., 2014. The Early Bronze Age Remains at Tell eṣ-Ṣāfi/Gath: An Interim Report. *Tel Aviv 41*(1), pp. 20-49.

Shugar, A.N. and Gohm, C.J., 2011. Developmental trends in Chalcolithic copper metallurgy: a radiometric perspective changed the world. In: Lovell, J.L., 2011 (Ed.), *Culture, chronology and the Chalcolithic: theory and transition*. Oxbow Books, pp.133-148.

Simmons, A.H., Rollefson, G.O., Kafafi, Z., Mandel, R.D., al-Nahar, M., Cooper, J., Köhler-Rollefson, I. and Durand, K.R., 2001. Wadi Shuʿeib, a Large Neolithic Community in Central

Jordan: Final Report of Test Investigations. *Bulletin of the American Schools of Oriental Research 321*, pp.1-39

Stuckenrath, R., 1963. University of Pennsylvania radiocarbon dates VI. *Radiocarbon 5*, pp.82-103.

Stuckenrath, R. and Ralph, E.K., 1965. University of Pennsylvania radiocarbon dates VIII. *Radiocarbon 7*, pp.187-199

Taylor, J.E., Rasmussen, K.L., Doudna, G., van der Plicht, J. and Egsgaard, H., 2005. Qumran textiles in the palestine exploration fund, London: Radiocarbon dating results. *Palestine exploration quarterly 137*(2), pp.159-167.

Toffolo, M.B., Arie, E., Martin, M.A., Boaretto, E. and Finkelstein, I., 2014. Absolute chronology of Megiddo, Israel, in the late Bronze and Iron Ages: high-resolution radiocarbon dating. *Radiocarbon 56*(1), pp.221-244.

Webster, L., 2015. Developing a radiocarbon-based chronology for Tel Azekah: the first stage.

Weinstein, J.M., 1984. Radiocarbon dating in the southern Levant. *Radiocarbon 26*(3), pp. 297-366.

Weinstein-Evron, M., Yeshurun, R., Kaufman, D., Eckmeier, E. and Boaretto, E., 2012. New 14 C dates for the Early Natufian of el-Wad Terrace, Mount Carmel, Israel. *Radiocarbon 54(*3-4), pp.813-822.

White, C.E., 2013. *The emergence and intensification of cultivation practices at the Pre-pottery Neolithic site of el-Hemmeh, Jordan: An archaeobotanical study*. Unpublished PhD dissertation. Boston University.

Time start BP	Time end BP	SPD of radiocarbon dates	Raw count	Aoristic weight	Randomised duration
11000	**9000**	0.67	0.40	0.40	0.70
10800	**8800**	0.67	0.41	0.41	0.28
10600	**8600**	0.67	0.28	0.28	0.14
10400	**8400**	0.62	0.37	0.37	0.24
10200	**8200**	0.58	0.29	0.29	0.28
10000	**8000**	0.49	0.35	0.35	0.24
9800	**7800**	0.41	0.45	0.45	0.21
9600	**7600**	0.21	0.40	0.40	0.10
9400	**7400**	-0.31	0.33	0.27	0.10
9200	**7200**	-0.37	0.22	0.14	0.05
9000	**7000**	-0.39	0.10	0.17	0.16
8800	**6800**	0.09	0.47	0.42	0.49
8600	**6600**	0.02	0.59	0.31	0.47
8400	**6400**	0.32	0.59	0.51	0.47
8200	**6200**	0.52	0.73	0.73	0.72
8000	**6000**	0.72	0.86	0.86	0.79
7800	**5800**	0.77	0.91	0.91	0.82
7600	**5600**	0.73	0.97	0.97	0.82
7400	**5400**	0.71	0.97	0.97	0.70
7200	**5200**	0.62	0.91	0.91	0.65
7000	**5000**	0.47	0.81	0.80	0.58
6800	**4800**	0.42	0.71	0.80	0.60
6600	**4600**	0.30	0.56	0.80	0.56
6400	**4400**	0.07	0.38	0.66	0.28
6200	**4200**	-0.42	0.38	0.65	0.26
6000	**4000**	-0.62	0.38	0.62	0.32
5800	**3800**	-0.54	0.36	0.32	0.32
5600	**3600**	-0.65	0.16	0.47	0.47
5400	**3400**	-0.50	0.26	0.40	0.47
5200	**3200**	-0.27	0.48	0.25	0.71
5000	**3000**	-0.09	0.55	-0.15	0.42
4800	**2800**	-0.32	0.22	-0.41	0.10
4600	**2600**	-0.41	0.12	-0.44	0.02
4400	**2400**		-0.10	-0.52	-0.09
4200	**2200**		-0.26	-0.50	-0.20
4000	**2000**		-0.35	-0.45	-0.21
3800	**1800**		-0.42	-0.52	-0.32
3600	**1600**		-0.36	-0.45	-0.28
3400	**1400**		-0.44	-0.50	-0.39
3200	**1200**		-0.24	-0.33	-0.18
3000	**1000**		-0.07	-0.24	0.03
2800	**800**		-0.36	-0.38	-0.24
2600	**600**		-0.45	-0.38	-0.28

Table S1. Spearman's correlations between all archaeological proxies and arboreal (tree) pollen (AP). Results for 200 year subsets of data in 2000-year moving time windows. The orange-blue scale values represent the statistical significance of correlation values, with orange representing $p<0.05$, red $p<0.01$, and blue $p<0.001$. Strongest cross-correlation (*lag -1; **lag -2; ***lag +1; no asterisk lag 0).

Time start BP	Time end BP	SPD of radiocarbon dates	Raw count	Aoristic weight	Randomised duration
11000	**9000**	-0.35	0.32	0.32	0.38
10800	**8800**	-0.43	0.41	0.41	0.38
10600	**8600**	-0.54	0.12	0.12	0.21
10400	**8400**	-0.65	0.07	0.07	-0.12
10200	**8200**	-0.37	0.29	0.29	0.03
10000	**8000**	-0.22	0.24	0.24	0.04
9800	**7800**	-0.16	-0.08	-0.08	-0.03
9600	**7600**	0.25	0.16	0.16	0.24
9400	**7400**	0.07	0.15	0.20	0.19
9200	**7200**	0.08	0.16	0.18	0.22
9000	**7000**	0.12	0.13	0.35	0.44
8800	**6800**	0.31	0.15	0.48	0.54
8600	**6600**	0.67	0.52	0.66	0.75
8400	**6400**	0.76	0.68	0.72	0.70
8200	**6200**	0.83	0.82	0.82	0.76
8000	**6000**	0.84	0.88	0.88	0.84
7800	**5800**	0.90	0.92	0.92	0.85
7600	**5600**	0.77	0.92	0.92	0.83
7400	**5400**	0.73	0.92	0.92	0.71
7200	**5200**	0.31	0.49	0.49	0.27
7000	**5000**	0.12	0.28	0.34	0.15
6800	**4800**	-0.04	0.07	0.15	-0.07
6600	**4600**	-0.36	-0.13	-0.16	-0.38
6400	**4400**	-0.36	-0.40	-0.51	-0.60
6200	**4200**	-0.12	-0.61	-0.61	-0.71
6000	**4000**	-0.05	-0.48	-0.50	-0.68
5800	**3800**	0.12	-0.16	-0.47	-0.59
5600	**3600**	0.27	0.31	-0.48	-0.59
5400	**3400**	0.33	0.53	-0.38	-0.20
5200	**3200**	0.48	0.78	-0.22	-0.10
5000	**3000**	0.19	0.57	-0.29	-0.16
4800	**2800**	0.01	0.46	-0.38	-0.31
4600	**2600**	-0.10	0.43	-0.31	-0.25
4400	**2400**		0.52	0.07	0.09
4200	**2200**		0.50	0.28	0.25
4000	**2000**		0.50	0.66	0.48
3800	**1800**		0.72	0.84	0.76
3600	**1600**		0.76	0.88	0.79
3400	**1400**		0.73	0.85	0.79
3200	**1200**		0.73	0.85	0.72
3000	**1000**		0.58	0.67	0.58
2800	**800**		0.65	0.71	0.64
2600	**600**		0.66	0.71	0.71

Table S2. Spearman's correlations between all archaeological proxies and OJCV (*Olea, Juglans, Castanea, Vitis*) pollen. Results for 200 year subsets of data in 2000-year moving time windows. The orange-blue scale values represent the statistical significance of correlation values, with orange representing $p<0.05$, red $p<0.01$, and blue $p<0.001$. Strongest cross-correlation (*lag -1; **lag -2; ***lag +1; no asterisk lag 0).

Time start BP	Time end BP	SPD of radiocarbon dates	Raw count	Aoristic weight	Randomised duration
11000	**9000**	0.03	0.40	0.40	0.16
10800	**8800**	-0.08	0.52	0.52	0.36
10600	**8600**	-0.37	-0.11	-0.11	0.12
10400	**8400**	-0.43	-0.12	-0.12	-0.05
10200	**8200**	-0.41	-0.06	-0.06	-0.15
10000	**8000**	-0.32	-0.10	-0.10	-0.03
9800	**7800**	-0.18	0.05	0.05	0.12
9600	**7600**	0.13	0.27	0.27	0.36
9400	**7400**	0.67	0.41	0.46	0.45
9200	**7200**	0.58	0.36	0.27	0.20
9000	**7000**	0.58	0.50	0.11	-0.04
8800	**6800**	0.56	0.41	0.20	0.01
8600	**6600**	0.58	0.29	0.33	0.08
8400	**6400**	0.19	-0.04	-0.02	0.03
8200	**6200**	0.22	0.08	0.08	0.15
8000	**6000**	-0.12	-0.23	-0.23	-0.16
7800	**5800**	-0.42	-0.55	-0.55	-0.43
7600	**5600**	-0.55	-0.77	-0.77	-0.62
7400	**5400**	-0.60	-0.80	-0.80	*-0.62
7200	**5200**	-0.59	-0.74	-0.74	-0.65
7000	**5000**	-0.64	-0.70	-0.75	-0.66
6800	**4800**	-0.62	-0.61	-0.75	-0.70
6600	**4600**	-0.52	-0.44	-0.75	*-0.65
6400	**4400**	-0.43	-0.24	-0.66	-0.55
6200	**4200**	-0.10	-0.14	-0.66	-0.48
6000	**4000**	0.05	-0.18	-0.71	-0.53
5800	**3800**	0.05	-0.30	-0.63	-0.49
5600	**3600**	0.13	-0.21	-0.50	-0.43
5400	**3400**	0.15	-0.24	-0.33	-0.38
5200	**3200**	0.05	-0.43	-0.19	-0.72
5000	**3000**	-0.15	-0.50	0.05	-0.54
4800	**2800**	0.21	-0.31	0.18	-0.41
4600	**2600**	0.44	-0.13	0.18	-0.28
4400	**2400**		0.16	0.64	0.16
4200	**2200**		0.33	0.58	0.26
4000	**2000**		0.41	*0.60	0.38
3800	**1800**		0.54	0.73	0.59
3600	**1600**		0.56	0.76	0.64
3400	**1400**		*0.64	0.81	0.73
3200	**1200**		0.58	0.75	0.58
3000	**1000**		0.09	0.20	0.18
2800	**800**		-0.08	-0.07	-0.04
2600	**600**		-0.12	-0.13	0.03

Table S3. Spearman's correlations between all archaeological proxies and API (Anthropogenic Pollen Index). Results for 200 year subsets of data in 2000-year moving time windows. The orange-blue scale values represent the statistical significance of correlation values, with orange representing $p<0.05$, red $p<0.01$, and blue $p<0.001$. Strongest cross-correlation (*lag -1; **lag -2; ***lag +1; no asterisk lag 0).

Time start BP	Time end BP	SPD of radiocarbon dates	Raw count	Aoristic weight	Randomised duration
11000	**9000**	-0.35	0.07	0.07	-0.01
10800	**8800**	-0.42	0.17	0.17	0.26
10600	**8600**	-0.58	-0.06	-0.06	0.15
10400	**8400**	-0.58	-0.08	-0.08	-0.08
10200	**8200**	-0.53	-0.17	-0.17	-0.24
10000	**8000**	-0.42	-0.18	-0.18	-0.13
9800	**7800**	-0.27	-0.23	-0.23	-0.02
9600	**7600**	0.15	0.12	0.12	0.32
9400	**7400**	0.64	0.23	0.27	0.45
9200	**7200**	0.52	0.20	0.06	0.19
9000	**7000**	0.59	0.31	0.16	0.21
8800	**6800**	0.59	0.18	0.28	0.30
8600	**6600**	0.59	0.09	0.38	0.36
8400	**6400**	0.18	-0.02	0.02	0.31
8200	**6200**	0.19	0.08	0.08	0.33
8000	**6000**	-0.02	-0.07	-0.07	0.20
7800	**5800**	-0.18	-0.26	-0.26	-0.03
7600	**5600**	-0.41	*-0.62	-0.62	-0.36
7400	**5400**	-0.48	*-0.73	-0.73	-0.41
7200	**5200**	-0.56	-0.78	-0.78	*-0.59
7000	**5000**	-0.53	-0.73	-0.75	*-0.60
6800	**4800**	-0.50	-0.63	-0.75	-0.65
6600	**4600**	-0.39	-0.46	-0.75	-0.62
6400	**4400**	-0.26	-0.24	-0.66	-0.54
6200	**4200**	-0.02	0.02	-0.52	-0.39
6000	**4000**	0.24	0.05	-0.47	-0.36
5800	**3800**	0.32	-0.01	-0.57	-0.33
5600	**3600**	0.36	0.27	-0.67	-0.45
5400	**3400**	0.33	0.26	-0.57	-0.32
5200	**3200**	0.37	0.24	-0.28	-0.56
5000	**3000**	0.08	0.10	-0.10	-0.49
4800	**2800**	0.12	0.13	-0.05	-0.38
4600	**2600**	0.18	-0.01	-0.20	-0.42
4400	**2400**		0.16	0.18	-0.08
4200	**2200**		0.20	0.41	0.07
4000	**2000**		0.26	0.47	0.19
3800	**1800**		0.43	0.64	0.42
3600	**1600**		0.42	0.66	0.47
3400	**1400**		0.56	0.77	0.65
3200	**1200**		0.42	0.66	0.49
3000	**1000**		0.02	0.16	0.15
2800	**800**		0.16	-0.04	0.04
2600	**600**		0.15	-0.07	0.15

Table S4. Spearman's correlations between all archaeological proxies and Regional pastoral indicator. Results for 200 year subsets of data in 2000-year moving time windows. The orange-blue scale values represent the statistical significance of correlation values, with orange representing $p<0.05$, red $p<0.01$, and blue $p<0.001$. Strongest cross-correlation (*lag -1; **lag -2; ***lag +1; no asterisk lag 0).

Time start BP	Time end BP	SPD of radiocarbon dates	Raw count	Aoristic weight	Randomised duration
11000	**9000**	0.42	0.39	0.39	0.22
10800	**8800**	0.42	-0.06	-0.06	-0.16
10600	**8600**	0.39	-0.09	-0.09	-0.15
10400	**8400**	0.54	-0.10	-0.10	0.21
10200	**8200**	0.26	-0.17	-0.17	0.10
10000	**8000**	0.22	0.04	0.04	0.09
9800	**7800**	0.09	0.02	0.02	-0.01
9600	**7600**	0.01	-0.02	-0.02	-0.01
9400	**7400**	0.22	0.16	0.10	0.24
9200	**7200**	0.38	0.03	0.23	0.30
9000	**7000**	0.42	0.23	0.42	0.41
8800	**6800**	0.55	0.24	0.50	0.44
8600	**6600**	0.64	0.26	0.58	0.47
8400	**6400**	0.66	0.67	0.61	0.56
8200	**6200**	0.62	0.58	0.58	0.58
8000	**6000**	0.66	0.60	0.60	0.65
7800	**5800**	0.55	0.38	0.38	0.38
7600	**5600**	0.38	0.36	0.36	0.31
7400	**5400**	0.12	-0.07	-0.07	0.02
7200	**5200**	0.41	0.26	0.26	0.33
7000	**5000**	0.33	0.29	0.26	0.43
6800	**4800**	0.50	0.45	0.47	0.62
6600	**4600**	0.60	0.45	0.53	0.73
6400	**4400**	0.60	0.39	0.53	0.77
6200	**4200**	0.55	0.09	0.33	0.61
6000	**4000**	0.47	0.17	0.51	0.62
5800	**3800**	0.52	-0.01	0.20	0.61
5600	**3600**	0.55	0.18	0.27	0.59
5400	**3400**	0.67	0.36	-0.09	0.58
5200	**3200**	0.64	0.52	0.27	0.37
5000	**3000**	0.48	0.45	0.26	0.39
4800	**2800**	0.15	0.32	0.12	0.22
4600	**2600**	-0.18	0.05	-0.07	0.01
4400	**2400**		-0.09	-0.29	-0.20
4200	**2200**		-0.10	-0.28	-0.21
4000	**2000**		-0.13	0.01	-0.12
3800	**1800**		0.02	0.19	0.13
3600	**1600**		0.03	0.21	0.10
3400	**1400**		-0.35	-0.18	-0.25
3200	**1200**		-0.58	-0.42	-0.35
3000	**1000**		-0.28	-0.12	-0.10
2800	**800**		-0.15	0.01	-0.01
2600	**600**		-0.12	0.01	0.02

Table S5. Spearman's correlations between all archaeological proxies and ruderal weeds + grazing resistant plants. Results for 200 year subsets of data in 2000-year moving time windows. The orange-blue scale values represent the statistical significance of correlation values, with orange representing $p<0.05$, red $p<0.01$, and blue $p<0.001$. Strongest cross-correlation (*lag -1; **lag -2; ***lag +1; no asterisk lag 0).

Time start BP	Time end BP	SPD of radiocarbon dates	Raw count	Aoristic weight	Randomised duration
11000	**9000**	-0.30	-0.22	-0.22	-0.52
10800	**8800**	-0.32	0.17	0.17	-0.24
10600	**8600**	-0.41	-0.36	-0.36	-0.38
10400	**8400**	-0.48	-0.36	-0.36	-0.65
10200	**8200**	-0.76	-0.52	-0.52	-0.70
10000	**8000**	-0.66	-0.40	-0.40	-0.71
9800	**7800**	-0.64	-0.57	-0.57	-0.76
9600	**7600**	-0.43	-0.34	-0.34	-0.55
9400	**7400**	-0.16	-0.19	-0.23	-0.36
9200	**7200**	-0.03	-0.06	0.13	0.03
9000	**7000**	-0.04	-0.02	0.27	0.26
8800	**6800**	0.16	0.25	0.30	0.30
8600	**6600**	0.04	0.19	0.15	0.14
8400	**6400**	0.32	0.41	0.40	0.14
8200	**6200**	0.32	0.33	0.33	0.02
8000	**6000**	0.22	0.26	0.26	-0.02
7800	**5800**	0.39	0.44	0.44	0.14
7600	**5600**	0.22	0.39	0.39	0.02
7400	**5400**	-0.02	-0.03	-0.03	-0.12
7200	**5200**	-0.16	-0.26	-0.26	-0.19
7000	**5000**	-0.35	-0.48	-0.46	-0.35
6800	**4800**	-0.37	-0.57	-0.45	-0.28
6600	**4600**	-0.62	-0.79	-0.64	-0.48
6400	**4400**	-0.38	-0.68	-0.51	-0.21
6200	**4200**	-0.01	-0.82	-0.60	-0.39
6000	**4000**	0.30	-0.84	-0.53	-0.41
5800	**3800**	0.47	-0.69	-0.33	-0.39
5600	**3600**	0.66	-0.47	-0.05	-0.14
5400	**3400**	0.64	-0.49	0.28	0.09
5200	**3200**	0.48	-0.41	0.01	0.19
5000	**3000**	0.50	-0.46	0.16	0.28
4800	**2800**	0.14	-0.72	-0.11	-0.09
4600	**2600**	0.05	-0.38	0.27	0.19
4400	**2400**		-0.07	0.40	0.28
4200	**2200**		0.10	0.36	0.33
4000	**2000**		0.16	0.39	0.39
3800	**1800**		0.18	0.42	0.35
3600	**1600**		0.13	0.38	0.27
3400	**1400**		-0.02	0.25	0.09
3200	**1200**		-0.13	0.14	0.03
3000	**1000**		-0.27	0.09	-0.19
2800	**800**		-0.12	0.09	-0.13
2600	**600**		-0.03	0.09	-0.01

Table S6. Spearman's correlations between all archaeological proxies and Simpson's Index. Results for 200 year subsets of data in 2000-year moving time windows. The orange-blue scale values represent the statistical significance of correlation values, with orange representing $p<0.05$, red $p<0.01$, and blue $p<0.001$. Strongest cross-correlation (*lag -1; **lag -2; ***lag +1; no asterisk lag 0).

Time start BP	Time end BP	AP sum	OJCV	API	Simpson's diversity	Regional pastoral	Ruderal weeds + grazing plants
11000	**9000**	0.56	0.12	0.32	-0.29	0.10	0.15
10800	**8800**	0.62	0.18	0.04	-0.16	-0.09	-0.09
10600	**8600**	0.54	-0.19	-0.36	-0.24	-0.35	-0.05
10400	**8400**	0.45	0.01	-0.50	-0.03	-0.55	-0.28
10200	**8200**	0.23	-0.09	-0.40	0.27	-0.59	-0.29
10000	**8000**	0.34	-0.09	-0.50	0.30	-0.72	-0.32
9800	**7800**	0.05	0.17	-0.47	0.59	-0.38	-0.39
9600	**7600**	-0.12	0.09	-0.59	0.48	-0.38	-0.38
9400	**7400**	-0.32	-0.12	-0.31	0.52	-0.21	-0.39
9200	**7200**	-0.10	0.15	-0.10	0.43	-0.30	0.08
9000	**7000**	-0.15	-0.08	-0.22	0.15	-0.27	-0.15
8800	**6800**	-0.55	-0.27	-0.27	0.12	-0.30	-0.22
8600	**6600**	-0.53	-0.58	-0.36	0.22	-0.43	-0.32
8400	**6400**	-0.72	-0.74	-0.29	-0.04	-0.46	-0.35
8200	**6200**	-0.66	-0.78	-0.24	-0.01	-0.49	-0.48
8000	**6000**	-0.52	-0.68	-0.15	0.01	-0.46	-0.49
7800	**5800**	-0.50	-0.56	0.07	-0.07	-0.26	-0.38
7600	**5600**	-0.21	-0.23	0.05	0.16	-0.26	-0.07
7400	**5400**	0.18	0.15	-0.12	0.16	-0.39	0.13
7200	**5200**	0.39	0.61	-0.29	0.24	-0.16	-0.24
7000	**5000**	0.38	0.60	-0.12	0.39	-0.09	-0.22
6800	**4800**	0.10	0.59	0.19	0.36	0.30	-0.37
6600	**4600**	0.33	0.38	-0.16	0.21	-0.01	-0.22
6400	**4400**	0.08	0.30	0.04	0.39	0.16	-0.28
6200	**4200**	0.03	0.49	0.03	0.56	-0.08	-0.08
6000	**4000**	-0.15	0.20	0.25	0.64	0.03	-0.04
5800	**3800**	0.03	0.31	0.21	0.60	0.10	0.14
5600	**3600**	-0.16	0.21	0.14	0.47	0.22	0.01
5400	**3400**	-0.15	0.04	-0.01	0.26	0.09	0.32
5200	**3200**	-0.03	0.18	-0.13	0.26	0.12	0.25
5000	**3000**	-0.01	0.18	-0.13	0.22	0.16	0.12
4800	**2800**	-0.03	0.03	-0.05	0.03	0.44	-0.08
4600	**2600**	-0.07	-0.21	0.38	-0.03	0.49	-0.59
4400	**2400**		-0.48	0.18	0.08	0.45	-0.55
4200	**2200**		-0.75	0.14	0.18	0.39	-0.58
4000	**2000**		-0.77	-0.31	-0.31	-0.03	-0.55
3800	**1800**		-0.78	-0.46	-0.55	0.04	-0.47
3600	**1600**		-0.80	-0.66	-0.58	-0.19	-0.35
3400	**1400**		-0.68	-0.51	-0.69	-0.12	-0.32
3200	**1200**		-0.59	-0.33	-0.69	-0.29	-0.48
3000	**1000**		-0.54	-0.23	-0.67	-0.18	-0.59
2800	**800**		-0.29	-0.19	-0.45	-0.07	-0.48
2600	**600**		-0.29	0.15	-0.45	0.04	-0.69

Table S7. Spearman's correlations between all pollen indicators and the climate proxy from Soreq's cave. Results for 200 year subsets of data in 2000-year moving time windows. The orange-blue scale values represent the statistical significance of correlation values, with orange representing $p<0.05$, red $p<0.01$, and blue $p<0.001$. Strongest cross-correlation (*lag -1; **lag -2; ***lag +1; no asterisk lag 0).

Time start BP	Time end BP	AP sum	OJCV	API	Simpson's diversity	Regional pastoral	Ruderal weeds + grazing plants
11000	**9000**	-0.08	0.65	0.64	-0.08	***0.65	-0.27
10800	**8800**	-0.30	0.82	0.71	0.30	***0.75	-0.72
10600	**8600**	-0.67	0.66	0.71	0.38	0.78	-0.70
10400	**8400**	-0.75	0.65	0.64	0.41	0.62	-0.77
10200	**8200**	-0.77	0.49	0.60	0.83	0.52	-0.71
10000	**8000**	-0.60	0.50	0.41	0.76	0.35	-0.53
9800	**7800**	-0.43	0.30	0.19	0.65	0.22	-0.35
9600	**7600**	-0.15	0.13	0.19	0.59	0.22	-0.28
9400	**7400**	0.19	0.32	-0.14	0.47	0.04	-0.25
9200	**7200**	0.31	0.08	-0.19	0.08	0.03	-0.37
9000	**7000**	-0.01	-0.24	-0.16	-0.09	-0.16	-0.32
8800	**6800**	0.01	-0.48	-0.42	-0.01	-0.45	-0.48
8600	**6600**	0.08	-0.49	-0.65	0.02	-0.55	-0.65
8400	**6400**	-0.43	-0.62	-0.54	-0.25	-0.31	-0.43
8200	**6200**	-0.73	-0.68	-0.37	-0.27	-0.09	-0.53
8000	**6000**	-0.88	-0.76	0.15	-0.22	0.26	-0.55
7800	**5800**	-0.90	-0.84	0.58	-0.54	0.35	-0.30
7600	**5600**	-0.94	-0.85	0.90	-0.48	0.77	-0.28
7400	**5400**	-0.94	-0.85	0.90	-0.04	0.83	0.15
7200	**5200**	-0.96	***-0.68	0.89	0.05	0.84	-0.03
7000	**5000**	-0.88	-0.66	0.89	0.25	0.76	-0.09
6800	**4800**	-0.82	-0.47	0.87	0.28	*0.72	-0.28
6600	**4600**	-0.71	-0.36	0.71	0.39	0.56	-0.22
6400	**4400**	-0.55	-0.20	0.61	0.08	0.37	-0.16
6200	**4200**	-0.44	-0.07	0.52	0.19	0.04	0.10
6000	**4000**	-0.33	-0.35	0.47	0.18	-0.07	-0.07
5800	**3800**	-0.25	-0.52	0.53	-0.05	-0.07	0.03
5600	**3600**	0.01	-0.71	0.43	-0.09	-0.07	-0.12
5400	**3400**	-0.04	-0.83	0.47	-0.07	-0.09	-0.35
5200	**3200**	-0.05	-0.87	0.33	0.15	-0.27	-0.66
5000	**3000**	-0.47	-0.84	0.49	0.33	-0.01	-0.67
4800	**2800**	-0.10	-0.48	0.16	0.75	-0.50	-0.41
4600	**2600**	0.04	-0.26	-0.16	0.53	-0.43	-0.08
4400	**2400**		-0.26	-0.24	0.30	-0.39	0.01
4200	**2200**		-0.42	-0.53	-0.02	-0.30	-0.01
4000	**2000**		-0.38	***-0.73	-0.22	-0.39	0.13
3800	**1800**		-0.36	***-0.67	-0.25	-0.26	0.12
3600	**1600**		-0.31	-0.42	-0.24	0.03	-0.16
3400	**1400**		-0.19	-0.19	-0.18	0.14	-0.12
3200	**1200**		-0.01	-0.08	-0.07	0.62	0.25
3000	**1000**		0.35	0.47	0.01	0.81	-0.14
2800	**800**		0.07	0.56	-0.20	0.68	-0.21
2600	**600**		-0.36	0.50	-0.61	0.45	-0.47

Table S8. Spearman's correlations between all pollen indicators and the climate proxy from Jeita's cave. Results for 200 year subsets of data in 2000-year moving time windows. The orange-blue scale values represent the statistical significance of correlation values, with orange representing $p<0.05$, red $p<0.01$, and blue $p<0.001$. Strongest cross-correlation (*lag -1; **lag -2; ***lag +1; no asterisk lag 0).

Time start BP	Time end BP	SPD of radiocarbon dates	Raw count	Aoristic weight	Randomised duration
11000	**9000**	0.50	0.70	0.70	0.87
10800	**8800**	0.57	0.53	0.53	0.79
10600	**8600**	0.54	-0.32	-0.27	0.70
10400	**8400**	0.18	-0.08	-0.08	0.17
10200	**8200**	-0.19	-0.41	-0.41	-0.19
10000	**8000**	-0.13	-0.23	-0.23	-0.22
9800	**7800**	-0.39	-0.52	-0.52	-0.53
9600	**7600**	-0.67	-0.70	-0.70	-0.73
9400	**7400**	-0.71	-0.73	-0.68	-0.93
9200	**7200**	-0.22	-0.59	-0.23	-0.53
9000	**7000**	-0.24	-0.49	-0.33	-0.62
8800	**6800**	-0.33	-0.42	-0.39	-0.71
8600	**6600**	-0.39	-0.39	-0.44	-0.78
8400	**6400**	-0.56	-0.60	-0.55	-0.75
8200	**6200**	-0.61	-0.55	-0.55	-0.68
8000	**6000**	-0.55	-0.46	-0.46	-0.55
7800	**5800**	-0.50	-0.43	-0.43	-0.46
7600	**5600**	-0.36	-0.12	-0.12	-0.22
7400	**5400**	-0.09	0.30	0.30	0.12
7200	**5200**	-0.05	0.27	0.27	0.10
7000	**5000**	-0.21	0.05	0.04	-0.08
6800	**4800**	-0.68	-0.40	-0.35	-0.37
6600	**4600**	-0.62	-0.36	-0.07	-0.20
6400	**4400**	-0.64	-0.63	-0.32	-0.49
6200	**4200**	-0.31	-0.70	-0.41	-0.53
6000	**4000**	0.05	-0.81	-0.49	-0.50
5800	**3800**	0.31	-0.48	-0.64	-0.35
5600	**3600**	0.45	-0.05	-0.64	-0.30
5400	**3400**	0.54	0.15	-0.60	-0.07
5200	**3200**	0.55	0.23	-0.50	-0.14
5000	**3000**	0.58	0.23	-0.41	-0.10
4800	**2800**	0.49	0.29	-0.32	-0.08
4600	**2600**	0.49	0.44	0.05	0.16
4400	**2400**		0.58	0.43	0.62
4200	**2200**		0.47	0.59	0.59
4000	**2000**		0.41	0.13	0.25
3800	**1800**		0.04	-0.22	-0.15
3600	**1600**		-0.19	-0.46	-0.33
3400	**1400**		-0.13	-0.40	-0.28
3200	**1200**		-0.15	-0.39	-0.35
3000	**1000**		0.01	-0.27	-0.24
2800	**800**		0.25	0.07	0.10
2600	**600**		0.23	0.07	-0.01

Table S9. Spearman's correlations between all archaeological proxies from Southern Levant and the climate proxy from Soreq's cave. Results for 200 year subsets of data in 2000-year moving time windows. The orange-blue scale values represent the statistical significance of correlation values, with orange representing p<0.05, red p<0.01, and blue p<0.001. Strongest cross-correlation (*lag -1; **lag -2; ***lag +1; no asterisk lag 0).

Time start BP	Time end BP	SPD of radiocarbon dates	Raw count	Aoristic weight	Randomised duration
11000	**9000**	0.31	0.81	0.81	-0.09
10800	**8800**	0.19	0.73	0.73	0.12
10600	**8600**	0.15	-0.32	-0.11	0.09
10400	**8400**	-0.27	-0.08	-0.44	-0.01
10200	**8200**	-0.26	0.06	0.06	-0.13
10000	**8000**	-0.12	-0.10	-0.10	-0.09
9800	**7800**	-0.02	-0.11	-0.11	-0.01
9600	**7600**	0.37	-0.44	-0.44	-0.28
9400	**7400**	0.21	-0.66	-0.66	-0.31
9200	**7200**	0.43	-0.87	-0.87	-0.56
9000	**7000**	0.58	-0.90	-0.90	-0.60
8800	**6800**	0.65	-0.95	-0.95	-0.60
8600	**6600**	0.65	-0.93	-0.93	-0.55
8400	**6400**	0.31	-0.54	-0.90	-0.10
8200	**6200**	0.36	-0.01	-0.92	-0.30
8000	**6000**	0.43	0.33	-0.93	-0.52
7800	**5800**	0.25	0.56	-0.93	-0.68
7600	**5600**	0.16	0.68	-0.93	-0.79
7400	**5400**	-0.24	0.26	-0.92	-0.72
7200	**5200**	-0.22	0.02	-0.94	-0.71
7000	**5000**	-0.37	-0.28	-0.91	-0.56
6800	**4800**	-0.39	-0.53	-0.87	-0.53
6600	**4600**	-0.28	-0.57	-0.78	-0.35
6400	**4400**	-0.32	-0.58	-0.65	-0.12
6200	**4200**	-0.33	-0.29	-0.26	0.20
6000	**4000**	-0.12	0.18	0.15	0.41
5800	**3800**	0.01	0.37	0.37	0.41
5600	**3600**	0.07	0.53	0.51	0.49
5400	**3400**	-0.18	0.41	0.61	0.59
5200	**3200**	-0.15	0.24	0.76	0.72
5000	**3000**	-0.35	0.19	0.69	0.62
4800	**2800**	-0.03	0.30	0.68	0.67
4600	**2600**	0.18	0.27	0.63	0.44
4400	**2400**		0.10	0.53	0.42
4200	**2200**		-0.14	0.15	0.32
4000	**2000**		-0.28	0.01	0.22
3800	**1800**		-0.31	-0.07	0.22
3600	**1600**		-0.31	-0.01	0.05
3400	**1400**		-0.20	0.07	0.21
3200	**1200**		0.04	0.19	0.21
3000	**1000**		0.39	0.12	0.21
2800	**800**		0.27	-0.13	-0.15
2600	**600**		0.25	-0.27	-0.08

Table S10. Spearman's correlations between all archaeological proxies from Northern Levant and the climate proxy from Jeita's cave. Results for 200 year subsets of data in 2000-year moving time windows. The orange-blue scale values represent the statistical significance of correlation values, with orange representing p<0.05, red p<0.01, and blue p<0.001. Strongest cross-correlation (*lag -1; **lag -2; ***lag +1; no asterisk lag 0).